TRIBHUVAN UNIVERSITY
INSTITUTE OF ENGINEERING
PULCHOWK CAMPUS

THESIS NO.:

Study of Surface roughness and its effect on Nusselt number of circular microchannel

by

Shuveksha Sapkota

A THESIS
SUBMITTED TO DEPARTMENT OF MECHANICAL AND AEROSPACE ENGINEERING IN PARTIAL FULFILLMENT OF THE REQUIREMENT FOR THE DEGREE OF MASTER OF SCIENCE IN
MECHANICAL SYSTEM DESIGN AND ENGINEERING

DEPARTMENT OF MECHANICAL AND AEROSPACE ENGINEERING
LALITPUR, NEPAL

MARCH, 2022

COPYRIGHT

TRIBHUVAN UNIVERSITY

INSTITUTE OF ENGINEERING

PULCHOWK CAMPUS

DEPARTMENT OF MECHANICAL AND AEROSPACE ENGINEERING

The undersigned certify that they have read, and recommended to the Institute of Engineering for acceptance, a thesis entitled " **Study of roughness and its effect on Nusselt number of circular microchannel**" submitted by Shuveksha Sapkota in partial fulfillment of the requirements for the degree of Master of Science in Mechanical Systems Design and Engineering.

_____

Supervisor, Assoc. Dr. Hari Bahadur Darlami

Asso. Professor, Department of Mechanical and Aerospace Engineering, Pulchowk Campus

_____

External Examiner, Er. Madan Timsina

Chief, NEA Subsidiary Company Monitoring Directorate

Nepal Electricity Authority

_____

Committee Chairperson, Dr. Surya Prasad Adhikari

Head, Department of Mechanical and Aerospace Engineering, Pulchowk Campus

Date: March 20, 2022

ABSTRACT

To ensure sustainability of energy system and to increase efficiency, miniaturization has been playing a major role these days. In current design scenario, high heat transfer rate using minimum pumping power are very important aspect. With respect to that, microchannel is characterized by flow and heat transfer in confined tiny geometries. This work represents the numerical simulation and analytical calculation performed in circular microchannels in order to study roughness and investigate its effect on the value of Nusselt number. The dataset of the available experimental investigations is cited and the study was performed with water as the working fluid and steel as the working medium while the Reynolds numbers has range from 400 to 3200. The surface roughness is studied that is generated through uniform distribution at the microscale. This research is mostly focused on Nusselt number and the simulation values was found to be 4.059,4.13466,5.08856 for smooth channel, channel with sand grain roughness, regular rough channel respectively. With an average error of 7.5%, the conventional co relation and simulation findings of Nusselt number are in agreement with each other.

ACKNOWLEDGEMENT

An exposure to detail study and research is always required for the enhancement of practical knowledge in this increasingly advancing and competitive scenario. I would like to acknowledge the opportunity provided by Department of Mechanical and Aerospace Engineering along with the continual support and guidance for conducting thesis research.

I owe special debt of gratitude to Asso. Prof. Dr. Hari Bahadur Darlami and Assistant Prof. Hari Bahadur Dura for their constant support and guidance throughout the implementation of the methodologies for this thesis. This research would not have been so fruitful and effective without the guidance of supervisors who were always ready for dealing with any of the queries and introducing about the new methodologies by providing valuable suggestions.

My special gratitude to Dr. Surya Prasad Adhikari, Head of Department of Mechanical and Aerospace Engineering, Pulchowk Campus for his constant encouragement. I express my profound sense of heartfelt appreciation to Program Coordinator Prof. Dr Er. Laxman Poudel the Department of Mechanical and Aerospace Engineering, Pulchowk Campus, IOE for providing us the necessary guidelines for thesis proposal as part of the syllabus for Masters of Science in Mechanical System Design and Engineering (MSMDE).

I also want to extend my regards to Nepal Academy of Science and Technology (NAST)for providing me the thesis grant for this research. The advice and information provided by the family, classmates and friends throughout the period has been a motivation to me and I highly appreciate this very welcoming nature and positive attitude.

Any further suggestions or criticisms for the improvement of this report will be highly appreciated.

Table of Contents

COPYRIGHT 2
APPROVAL PAGE 3
ABSTRACT 4
ACKNOWLEDGEMENT 5
LIST OF TABLES 8
LIST OF FIGURES 9
LIST OF ABBREVIATIONS 11
LIST OF SYMBOLS 12
CHAPTER ONE: INTRODUCTION 13
1.1 BACKGROUND 13
1.1.1 Microchannel 13
1.1.2 Surface roughness 15
1.3 Problem statement 18
1.4 OBJECTIVES 19
1.4.1 Main Objective 19
1.4.2 Specific objectives 19
CHAPTER TWO: LITERATURE REVIEW 20
CHAPTER THREE: RESEARCH METHODOLOGY 23
3.1 Data set description 24
3.2 Analytical calculation 24
3.3 Software simulation 26
3.4 Governing equation 26
3.5 CFD Analysis of the microchannel 28
3.5.1 Geometry and meshing 28
3.5.2 Mesh Independence Test 28
3.5.3 Physics setup 29
3.5.4 Post processing and results 29
3.6 Case Studies 30
3.6.1 Case Study 1: Smooth microchannel 30
3.6.2 Case Study 2: Microchannel with Sand grain roughness 32
3.6.3 Case Study 3: Single Regular Rough microchannel 34
3.6.4Case Study 4: Random Rough Microchannel 36
CHAPTER FOUR: RESULTS AND DISCUSSION 38
4.1 Results from simulation 38

4.1.1 Smooth microchannel 38
4.1.2 Microchannel with sand grain roughness 38
4.1.3 Single regular rough microchannel 38
4.1.4 Random Rough microchannel 39
4.2 Performance Parameters 49
CHAPTER FIVE: CONCLUSIONS AND RECOMMENDATIONS 53
5.1 Conclusions 53
5.2 Recommendations 53
REFERENCES 54
APPENDIX A: DATA GENERATION OF ROUGH CHANNEL 56
APPENDIX B: MATLAB CODES 59

LIST OF TABLES

Table 3.1Data details of the circular microchannel[26].....24
Table 4.1 Summary of values.....49

LIST OF FIGURES

Figure 1.1 Blood Sample cartridge using microfluidic channels(Gad-el-Hak, and Seemann, 2002).....14
Figure 1.2Micro heat exchanger from rectangular channels machined in metal. (Gad-el-Hak, and Seemann, 2002).....15
Figure 1.3 Enlarged view of microtubes (Yang et al. 2012).....16
Figure 1.4 Sand-grain height for a uniform sand-grain roughness(Hetsroni et al. 2011).....16
Figure 3.1 Flowchart of methodology.....23
Figure 3.2Mesh Independence Test.....29
Figure 3.3Front view of the circular microchannel.....30
Figure 3.4Structured mesh (Isometric view).....31
Figure 3.5Full cross section of microchannel (Isometric View).....32
Figure 3.6Construction of fifteen microchannel in Solidworks.....34
Figure 3.7 Regular Rough Tube.....35
Figure 3.8 Mesh Generation of Rough microchannel.....35
Figure 4.1Roughness Profile for M=2, N=16, β =0.5.....39
Figure 4.2 Roughness Profile for M=16, N=16, β =5.....40
Figure 4.3 Roughness Profile for M=16, N=16, β =1.....40
Figure 4.4 Roughness Profile for M=10, N=16, β =0.5.....41
Figure 4.5 Roughness Profile for M=16, N=2, β =0.5.....41
Figure 4.6 Roughness Profile for M=16, N=10, β =0.5.....42
Figure 4.7 3D Cylindrical Surface with 1 % radius variation.....43
Figure 4.8 Cross Sectional Area of Cylindrical Surface for 1 % radius Variation.....43
Figure 4.9 3D Cylindrical Surface with 2 % radius variation.....43
Figure 4.10 Cross Sectional Area of Cylindrical Surface for 2 % radius variation.....43
Figure 4.11 3D Cylindrical Surface with 3 % radius variation.....44
Figure 4.12 Cross Sectional Area of Cylindrical Surface for 3 % radius Variation.....44
Figure 4.13 3D Cylindrical Surface with 4 % radius variation.....44
Figure 4.14 Cross Sectional Area of Cylindrical Surface for 4 % radius Variation.....44
Figure 4.15 3D Cylindrical Surface with 5 % radius variation C.....45
Figure 4.16 Cross Sectional Area of Cylindrical Surface for 5 % radius Variation.....45
Figure 4.17 3D rough microchannel.....46
Figure 4.18 Meshing of the rough microchannel.....46

Figure 4.19 Temperature contour at inlet side 47
Figure 4.20 Temperature vs length along the channel for five locations 47
Figure 4.21 Velocity contour at the inlet side of the channel 48
Figure 4.22 Velocity contour along the axial length of the channel 48
Figure 4.23 Graph showing Nu vs Re with simulation data and polynomial model 50
Figure 4.24 Graph showing error between simulated and Fitted value 51
Figure 4.25 Graph of Nu vs Re of calculated and simulated data 51

LIST OF ABBREVIATIONS

CFD	-	Computational fluid dynamics
IOE	-	Institute of Engineering
MEMS	-	Micro-electromechanical systems
Pa	-	Pascal
RMSE	-	Root mean square error
SIMPLE	-	Semi-Implicit Method for Pressure Linked Equation
VLSI	-	Very Large Scale Integration

LIST OF SYMBOLS

A	Area of heat transfer
A_c	Circular cross-section area
cp	Specific heat
D_i	Internal diameter
f	friction factor
Gz	Graetz number
h	Heat transfer coefficient
K	conductivity of water
L	Length of the channel
V	Velocity
$\dot{m}$	mass flow rate
Nu_d	Nusselt number
Pr	Prandtl number
q	Heat transfer rate
$\ddot{q}$	Heat flux
Ra	Average roughness
Re_d	Reynolds number
T_i	Inlet water temperature
T_x	Local water temperature
T_{wx}	Local tube inside wall temperature
x	Axial position of tubes
μ	Viscosity

CHAPTER ONE: INTRODUCTION

1.1 BACKGROUND

The quest for alternative energy resources has become the major concern in the area of energy conservation in this era. This conservation has been important as the energy sources have been depleting day after another. Thus, to ensure sustainability of these energy system and increasing efficiency, miniaturization has been playing a major role. Miniaturization in manufacturing and electromechanical systems, according to studies, have the potential to become "economic drivers" in the near future(Ameel et al., 1997). Characterized by flow and heat transfer in confined tiny geometries, miniaturization has captured the heat exchanger technology also. As we know heat exchangers are inherently a crucial part of the systems involving heat and mass transfer, their efficiency contributes to overall system efficiency. They are mostly used in the industries like microelectronics, aerospace, biomedical, robotics, cooling of gas turbine blades, power and process industries, fuel cell systems, advanced heat sink design, refrigeration and air conditioning, tele communications, powerful laser mirrors, infrared detectors, and automotive.

1.1.1 Microchannel

Micro channel heat exchanger is a type of heat exchanger in which fluid flows in lateral confinements with dimension below 1mm(Swift et al., 1985).The fundamental benefit of adopting microchannel is that it has a high area to volume ratio, which results in a high convective heat transfer coefficient rate. Uneven flow distribution, pressure drop, and heat transfer rate are still some of the obstacles and limitations in increasing its performance. The pressure drop will increase as the channel diameters are reduced to micro-scale(Fung & Majnis, 2019). As the dimension is reduced, flow in microchannel differs from the macroscopic scale because the small scale makes molecular effects predominant and also amplifies the magnitudes of some ordinary continuum parameters to extreme levels. The thermal contact resistance at the interface of a heat-generating component and a heat sink can be minimized by integrating these micro channels directly within the heat-generating component. Furthermore, because of this property, micro channels have lower substrate temperatures and smaller temperature gradients, making them

appealing for microelectronics cooling applications. Our main target is to make pressure drop minimum and heat transfer rate maximum.

Figure 1.1 Blood Sample cartridge using microfluidic channels(Gad-el-Hak, & Seemann, 2002)

Several investigations in microchannel show that thermal and hydrodynamic performance is different from that of macro channels and these discrepancies may have been caused due to factors ignored in them. One of the most important of these, surface roughness, is of more concern. Almost in all types of flow systems, rough walls exist which may either lead to improvement or deterioration of the desired functionality. To promote mixing of fluid, wall roughness can be increased whereas to eliminate the flow disturbances, it is to be decreased.

The Nusselt number for thermally completely developed flow is only dependent on the cross-sectional form of the channel, according to the traditional theory of internal laminar heat transfer. However, with the current rapid development of microfluidic devices, the channel scale will continue to shrink, and the relative importance of channel surface roughness will become more of a concern and consequence. Recent research has focused on whether roughness has an effect on micro internal laminar heat transmission and whether the Nusselt number in rough micro channels is still solely determined by the cross-sectional form of the channel(Kandlikar, 2008)(Sobhan & Garimella, 2001).

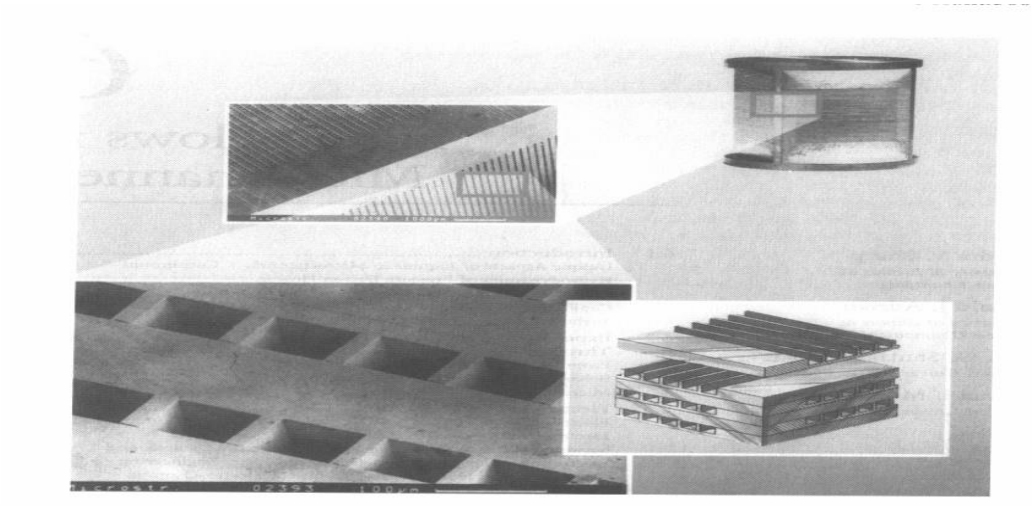

Figure 1.2 Micro heat exchanger from rectangular channels machined in metal. (Gad-el-Hak, & Seemann, 2002)

For the heat transfer characteristics, Nusselt number also increases with increasing Reynolds number and the contribution to higher Nusselt number is seen if larger roughness exists. The local Nusselt values following the entrance region are no longer constant because of the roughness, and they tend to fluctuate along rough microchannels. Furthermore, rough microchannels perform better in terms of global heat transport than smooth microchannels. This roughness is seen as the manufacturing techniques like micromechanical machining, X-ray machining, micro drilling, photolithographic based methods are used.

1.1.2 Surface roughness

The Darcy friction factor is plotted as a function of Reynolds number and relative roughness on the Moody Chart, one of the most important tools in fluid mechanics. The data was collected by coating the interior surfaces of roughened pipes with a monolayer of sand and calculating pipe wall roughness as the average diameter of sand grains(T. Adams & Grant, 2012).

Surface roughness has a big impact on engineering issues and causes more turbulence near rough walls. Additionally, it has an effect on raising wall shear stress. The ability to accurately estimate near-wall flows is dependent on a number of factors. Hence, Surface roughness should be properly modeled. In CFD analysis, surface roughness can be considered using special parameter known as sand grain roughness that depend not only on roughness amplitude, but also on shape and frequency.

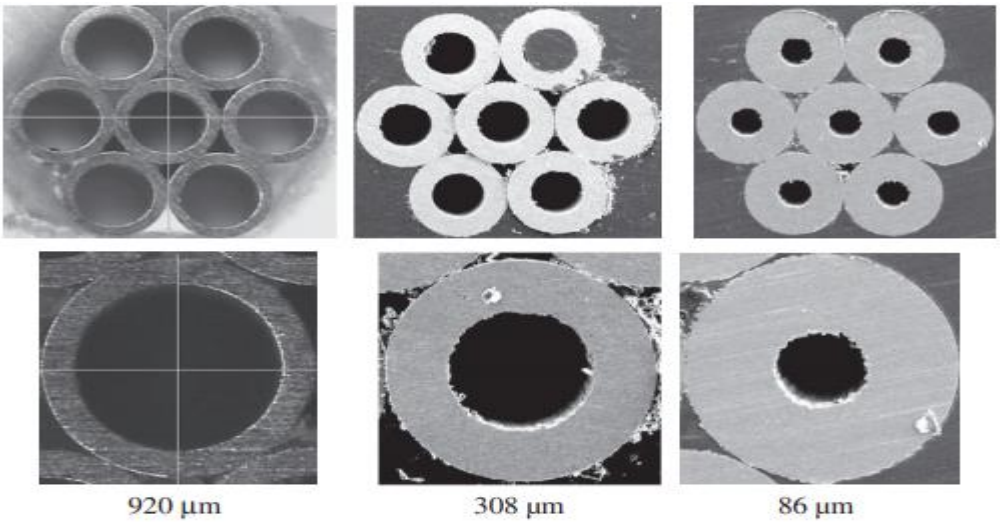

Figure 1.3 Enlarged view of microtubes (C. Y. Yang et al., 2012)

The logarithmic profile exists for rough walls, but towards the wall, the near wall treatment becomes more complicated. It depends on two variables namely the dimensionless wall distance y+ and height of roughness (Ra).The arithmetic average of absolute roughness, which, like the wall border, must be given.

Nikuradse, who studied the hydraulic effects of consistent sand particle roughness on cylindrical pipe flow in the 1930s, named as sand grain roughness. Because the equivalent sand roughness is determined by the arrangement (pattern), distance (density), and form of roughness components such as grooves, sand grains, waves, and cuboids, these elements may differ in roughness while having the same geometrical roughness height k. Roughness components in the shape of plates, for example, are roughly the same height as sand grains.

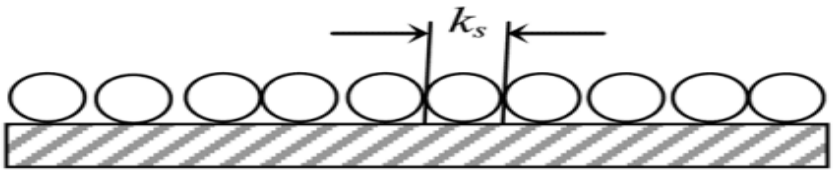

Figure 1.4 Sand-grain height for a uniform sand-grain roughness(Hetsroni et al., 2011)

For this model, two parameters namely roughness height (Ks) and roughness constant is considered. Roughness height is a representative distance to the wall and the value of zero denotes smooth surfaces. Ks is easy to produce when the sand particle roughness is consistent, as seen above. The user can specify Ks based on average values for

unusual grain sizes. The other parameter, roughness constant is a metric measuring how consistent the roughness is. The number of inputs might range from 0.5 to 1. A roughness of 0.5 implies consistent wall roughness. The roughness is severely non-uniform, both in terms of spacing and height, with a value of 1. In certain situations, the wall roughness will be quite uneven and will not resemble sand particle. Users should calculate the comparable sand-grain roughness in this case.

Many commercial software packages provide this feature with the roughness equivalent to sand grains. It's crucial to remember that the roughness of the sand grain is significant. So the geometric roughness of the surface is not equal to the sand grain roughness height(Muhič & Mitruševski, 2017).

1.3 Problem statement

High heat transfer rates with little pumping power and space are significant aspects of current design concepts. The introduction of a disturbance in the flow is one technique to boost the heat transfer rate with low conductivity fluids, but this results in an increase in pumping power, which is undesirable. Another option is to optimize the geometry. Regardless, increasing the heat transfer coefficient by reducing the hydraulic diameter of the channel or employing rough channels is the greatest technique to improve heat transfer rate.

Moreover, the channel geometry and entrance cross section has significant effect on the flow and heat characteristics effectiveness, heat transfer rate, pressure drop along with hydraulic and thermodynamic performance of microchannel. Various kinds of geometry like rectangular, trapezoidal, circular, triangular, wavy, irregular etc. has been used in the research works. Since our main target is to increase the heat transfer rate with low pumping power and to keep pressure drop to minimum, several researchers have performed experimental, analytical and numerical modeling with respect to channel geometry. Among all kinds of geometry studied and mentioned, it has been found that circular geometry gives the highest effectiveness due to increase of effect of axial conduction with low pumping power and high heat transfer rate. Moreover circular geometry gives high performance index for the flow with low Reynolds number. There is significant amount of pressure drop which may be due to early transition from laminar to turbulent flow or the effects of surface roughness as the value of Reynolds number increases.

We ignore any other possible justification of divergence from macroscale flow behavior because our major goal is to isolate this particular aspect of the problem: consequently, we don't account for viscous dissipation and solve the equations for laminar flow of an incompressible fluid with constant characteristics. Many researchers have conducted experiments on roughness in microchannels in the past, with the majority of the investigations focusing on the comparison of smooth and rough channels.

The numeric method is still commonly employed separate from the experimental process. A regular rough element method and a random roughness method are the two basic approaches to modeling a rough surface. The cuboid, pyramid, or other

regular impediments are placed on a smooth surface to create a rough surface using the regular rough element method. Because this method is simple to apply, several researchers have selected it to model roughness.The regular element approach is a simple way to model a rough surface, but heat transfer and fluid flow are highly dependent on the parameters of roughness components and geometry shapes necessitating the consideration of a large number of parameters. As a result, some researchers looked for a better way to model random roughness. The physical characteristics of roughness are considered in the random roughness method, which is closer to real roughness than regular roughness(Lu et al., 2020).

The superimposition of a different formed imperfection on the ideal smooth wall may also be used to simulate roughness. To obtain a more accurate roughness modeling, the heights of the imperfections are randomly created.

1.4 OBJECTIVES

1.4.1 Main Objective

The main objective of this work is to study surface roughness and its effect on Nusselt number of circular micro channel.

1.4.2 Specific objectives

- To simulate the effectiveness of Nusselt number due to roughness with different cases
- To generate and study the nature of surface roughness on the channel using Gaussian distribution
- To construct and select the proper roughness modelling technique
- To compare and validate the results from numerical simulation.

CHAPTER TWO: LITERATURE REVIEW

Years ago, the first application of miniaturization for heat removal was presented in a paper titled "High Performance Heat Sinking for VLSI," which is considered as the first study on microchannel heat transfer. Many studies have followed in the footsteps of this pioneering study, and microchannel flow has been recognized as a high-performance heat removal method ever since(Tuckerman & Pease, 2013).

The experiment on microtubes with diameters ranging from 50um to 254um have been performed and the results deviated from conventional theory of friction factor and other flow charactersistics in laminar region . Also the laminar to turbulent flow was observed at Reynolds number between 300 and 900(Dongqing & Mala, 1999).

The numerical simulation was carried out which concluded that the thermal conductivity ratio, hydraulic diameter and Reynolds number affect the behaviour of axial heat conduction.Also, by employing porous fins, it improves heat transfer performance as well as the water in microchannels mechanism, lowering the pressure drop(Hasan et al., 2014).

The pressure drop and heat transfer characteristics of air flow in microtubes was carried out where the surface roughness has also been considered with different value.The experimental results reveal that when the influence of gaseous flow compressibility is adequately taken into account, the frictional coefficient of gas flow in microtubes is the same as that in larger tubes(C. Y. Yang et al., 2012).

An experiment in which the flow behaviors for air flow were investigated in microchannels with rectangular cross sections. Different roughness values were used, and the results showed that roughness with a higher value tends to have a higher Poiseuille number(Liu et al., 2015).

The influence of surface roughness on heat transfer in micro-channels was numerically investigated, and it was discovered that the Nusselt number grows with increasing relative surface roughness in laminar flow. The Nusselt number for turbulent flow increases as the relative surface roughness of the tubes increases(Koo & Kleinstreuer, 2005).

High relative roughness of the walls improves convective heat transfer because the thermal boundary layer regenerates. Surface roughness effects were associated

with lower Nusselt number value when comparing experimental data to numerical results obtained solving a conjugate heat transfer problem(Peiyi & Little, 1983).

The effect of wall roughness on fluid flow and heat transmission in microchannels was investigated using a model. Roughness has a favorable impact on thermal performance and flow resistance, according to findings(Guo et al., 2015).

The findings of experimental research on microchannel heat transfer and fluid flow characteristics are varying and one can come to a conclusion that the results are highly scattered. This is particularly problematic in the case of heat transfer effects. In the so-called microchannel heat sink, for example, there is an optimum channel size, and the optimization result is highly influenced by the heat transfer characteristics of microchannels. As a result, the study of single-phase microtube heat transfer was initiated(Lelea et al., 2004).

Because of small hydraulic diameters, microchannels have extremely high heat transfer coefficients. An alternate method for forecasting the average Nusselt Number in circular microchannels when the flow is fully developed has been used and the results of this research are derived as the equations for the average Nusselt Number under the different condition of the flow(Khan et al., 2010).

As we know Nusselt numbers with various roughness characteristics differ for the same Reynolds number. Nusselt number grows considerably with Reynolds number in laminar and turbulent regimes. With a rise in Reynolds number in some test pieces, the rate of growth for Nusselt numbers slows in the transition regime. Further the experimental Nusselt number is lower than the original value, according to the results. The reasons for divergence can be deduced from the definition, which states that the inner wall temperature is the theoretical Nu wall temperature. Because the inner wall temperature is more difficult to assess in practice, the outer wall temperature is used in this article. Further the small diameter of the circular microchannel makes it difficult to ensure microchannel being a theoretical circle and experimental Nusselt number may be affected by entrance effect. However the overall performance does not change much and one explanation for this might be that an increase in roughness reduces flow area for the same mass flow rate, resulting in higher flow velocity and lower value of heat exchange efficiency(Xing et al., 2016).

The heat transfer experiments with R114 and water with tube diameters ranging from 130-290um in capillary tubes. Direct condensation on the tube's outside

surface heated the microtubes. Conventional correlations discovered for laminar and turbulent flows was compared with experimental findings. They came to the conclusion that traditional models for forecasting heat transport in microtubes were insufficient(Celata et al., 2004).

Using direct surface roughness measurements in fluid flow calculations may result in considerable inaccuracy. A basic method used to solve a variety of problems has been described where the surface roughness characteristics can be translated to sand-grain roughness equivalents. For almost any surface, the method was used to convert the roughness value to comparable sand-grain roughness. When compared to raw roughness value, the method gives greater agreement with fluid flow tests (T. Adams & Grant, 2012).

Previous investigations in single-phase heat transfer in micro-channels, on the other hand, have found a lot of inconsistency with classical behavior. So yet, no definite conclusion has been reached about the adherence to macro-scale behavior. Necessitating this discrepancy, existing experimental studies has been reviewed and analysed. Recent studies reveal laminar and turbulent regimes in microtubes match classical correlations rather well. The impact of heat-flux magnitude, diameter, roughness can't be ignored. As a result, this research has been unable to come up with a solid conclusion that encompasses all of the experimental, numerical, and analytical findings (Krishnamoorthy & Ghajar, 2014).

The heat transfer properties of turbulent, single-phase forced convection of water in micro-channels with diameters of 760m and 1090m was studied. The Nusselt values were found to be greater than those anticipated by traditional correlations. Furthermore, the investigators discovered that the divergence in the results grew as the tube diameter and Reynolds number decreased. The existing Gnielinski corelation has been modified to address the Nusselt number for small diameter tubes(T. M. Adams et al., 1997).

Water flowing in micro-tubes was studied for flow characteristics and forced convective heat transfer. For the computation of heat transfer coefficients, conventional correlations were insufficient. In the laminar regime, the heat transfer coefficient was found to be greater whereas the fluctuation was modest in the turbulent regime(Celata & Cumo, 2003) .When compared to the larger micro-tube, the smaller micro-tube showed a greater deviation but in better agreement with (T. M. Adams et al., 1997).

CHAPTER THREE: RESEARCH METHODOLOGY

This chapter details the methodology that is used throughout the thesis, from the beginning till the end of this thesis. The data has been referenced through experimental research paper which is then followed by analytical calculations where the parameters and equations are applied in order to calculate and validate the results from the simulation. The geometry has been prepared either on software Solidworks or Ansys Design Modeler as per the case. As the research is based on a CFD flow analysis, followed by geometry setup, mesh generation, physics setup and post processing, the simulation was carried out in Ansys where every case has been evaluated. Since the main target is the study of roughness and its behaviour, roughness modeling has been done through Gaussian distribution by programming in MATLAB. Finally, the results have been verified from the numerical simulations.

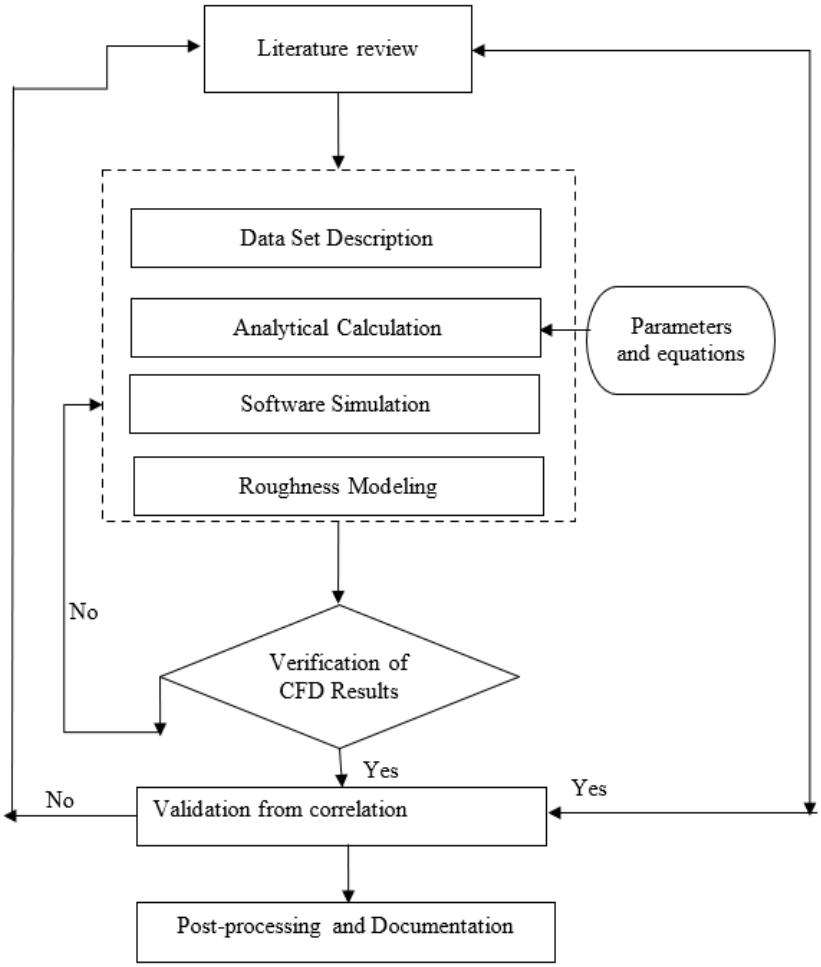

Figure 2.1 Flowchart of methodology

3.1 Data set description

This thesis is conducted by undertaking experimental research performed on topic " Heat transfer characteristics of water flow in microtubes" by (C. Yang & Lin, 2007) , an efficient model where the findings of the tests demonstrate that conventional correlations for laminar and turbulent flow may be used to accurately predict fully developed heat transfer performance in microtubes. Due to the difficulty and unavailability of MEMS fabrication technology, no experimental analysis has been done for now for this research.Therefore this work incorporates modeling of roughness by constructing the rough microchannel geometry to observe the effects of roughness particularly focused on Nusselt number.

Table 2.1 Data details of the circular microchannel(C. Yang & Lin, 2007)

S.N.	Particulars	Values
1.	Inner diameter of microchannel	123 μm
2.	Outer diameter of microchannel	282 μm
3.	Length of microchannel	140mm
4.	Heating length	120mm
5.	Fully developed length	75mm
6.	Average Roughness	1.4μm
7.	Standard Deviation	1 μm
8.	Number of tube measured	15
9.	Transition Reynolds number	2300-3000

3.2 Analytical calculation

The convective heat transfer characteristics in circular microchannel can be derived from the following equations.

Heat transfer area is given by,

$$A = \pi \times \mathrm{Di} \times \mathrm{L} \qquad (3.1)$$

where, Di = internal diameter

L = length of tube.

Tube cross section area is given by,

$$Ac = \pi \times \frac{\mathrm{Di}^2}{4} \tag{3.2}$$

Flow velocity is given by,

$$V = \frac{Re \times \mu}{\rho \times Di} \tag{3.3}$$

Where, Re= Reynolds number
μ = dynamic viscosity

Mass flow rate is given by,

$$\dot{m} = Ac \times V \times \rho \tag{3.4}$$

Further, We can estimate Tx, at position x from heating entrance by,

$$\frac{qx}{\mathrm{L}} = \dot{m}cp\ (Tx - Ti) \tag{3.5}$$

From law of convection,

$$\ddot{q} = \frac{\mathrm{q}}{\mathrm{A}} = h\ (Twx - Tx) \tag{3.6}$$

We have to determine Prandtl number as,

$$Pr = \mu\mathrm{cp}/\mathrm{k} \tag{3.7}$$

Shah and Bhatti presented a set of correlations to calculate the value of local Nusselt number of thermally developing laminar flow in a circular tube across a wide range of Graetz numbers (Gz).

Graetz number is given by (C. Yang & Lin, 2007),

$$Gz = \frac{\mathrm{Red} \times \mathrm{Pr} \times \mathrm{Di}}{\mathrm{x}} \tag{3.8}$$

As per criterion meet my calculation of Graetz number, if 1/Gz ≥0.0015 we have(C. Yang & Lin, 2007),

$$Nu_d = 4.364 + 8.68(10^{-3}Gz)^{0.506}\exp(-\frac{41}{Gz}) \quad (3.9)$$

The flow regime shifts to turbulent about Reynolds numbers of 2300–3000. Thus the turbulent Nusselt numbers are exactly the same as those anticipated for $3000<Re<5*10^6$ by the Gnielinski correlation (Lin & Yang, 2007) mentioned as,

$$Nu_d = \frac{\left(\frac{f}{8}\right)(Re-1000)Pr}{1+12.7\left(\frac{f}{8}\right)^{\frac{1}{2}}\left((Pr)^{\frac{2}{3}}-1\right)} \quad (3.10)$$

$$\text{where } f = (1.82\ln(Re)-1.64)^{-2} \quad (3.11)$$

3.3 Software simulation

The research also encompasses the detailed CFD analysis. The CFD analysis will be conducted through the use of CFD software namely: ANSYS Fluent which will be utilized to run simulations. Since there will be many simulation cases, computational time will be high.

3.4 Governing equation

The entire Navier-Stokes equations must be simulated for varied fluid flows in a variety of engineering situations. Various scholars have suggested and created a number of different algorithms. However, there has yet to be created a truly robust approach in terms of numerical and modeling accuracy as well as efficiency. Hence the existing Navier-Stokes equations algorithms may be divided into two categories: density-based approaches and pressure-based approaches. The calculation of velocity field is done using the equations of momentum for each of these approaches.

For our study, we are using water as the flow fluid. So for the incompressible flow domain, pressure-based techniques are being developed. The pressure field is obtained by modifying the continuity and momentum equations to construct a pressure correction

equation. Because the solution process is traditionally sequential, it can handle a larger number of equations depending on the physics of the problem.

The continuity equation, momentum equation, and energy equation are all part of the single phase model equations. The continuity and momentum equations are used to derive the velocity vector. The energy equation is used to compute the temperature distribution and wall heat transfer coefficient. The continuity equation, often known as the mass conservation equation, is written as follows,

Mass conservation equation

$$\frac{\partial \rho}{\partial t} + \nabla.(\rho \vec{v}) = S_m \tag{3.12}$$

The mass conservation equation, in its general form, is applicable for both compressible and incompressible flows. The mass contributed to the continuous phase from the dispersed second phaseand any other user-defined sources is referred as the source mentioned above.

Momentum conservation equation

$$\frac{\partial}{\partial t}(\rho \vec{v}) + \nabla.(\rho \vec{v}\vec{v}) = -\nabla p + \nabla.(\bar{\bar{\tau}}) + \rho \vec{g} + \vec{F} \tag{3.13}$$

where,

p= Static Pressure

$\rho \vec{g}$ = Gravitational force

$\vec{F}$ = Other model-dependent source terms, such as porous-media and user-defined sources

$\bar{\bar{\tau}}$ = Stress Tensor

Energy equation

$$\frac{\partial}{\partial t}(\rho E) + \nabla.(\vec{v}\,(\rho E + p)) = \nabla.\left(\mathrm{K}_{eff}\nabla T - \sum_j h_j \overrightarrow{J_j} + (\bar{\bar{\tau}}_{eff}\,.\,\vec{v})\right) + S_h \tag{3.14}$$

where,

K_{eff}= effective conductivity (K+K_t) and K_t signifies turbulent thermal conductivity as per turbulence model used

$\vec{J_J}$ = Representation of diffusion flux of species J

The energy transfer owing to conduction, species diffusion, and viscous dissipation are represented by the first three terms on the right hand side, respectively.

3.5 CFD Analysis of the microchannel

The research was based on a CFD flow analysis, followed by geometry setup, mesh generation, physics setup, as detailed in the parts that follow:

3.5.1 Geometry and meshing

According to the specifications, the circular microchannel geometry was created. The hydraulic diameter was utilized to build the microchannel geometry, allowing them to be prepared in millimeter dimensions. For the rough microchannel geometry, it was constructed in Solidworks and imported to ANSYS. Then meshing was then carried where the various methods of meshing was tried and among all of them the effective one was choosen that yielded better results.

3.5.2 Mesh independence test

The graph illustrating resultant value and number of cells in simulation is the easiest technique to verify for a mesh independent solution. Three types of mesh like fine, coarse and medium were considered in meshing section. This is shown in the diagram below, where we have three values for the Nusselt number at an outlet. We can see that result that might be considered "converged" for that particular mesh but it can be noticed that value rised which is not within user defined tolerance by raising the mesh resolution to more elements.

So as per the grid convergence analysis the number of nodes for perfect mesh was set to be around 1,06,7,009 since further refinement in the mesh would have only increased the computational time.

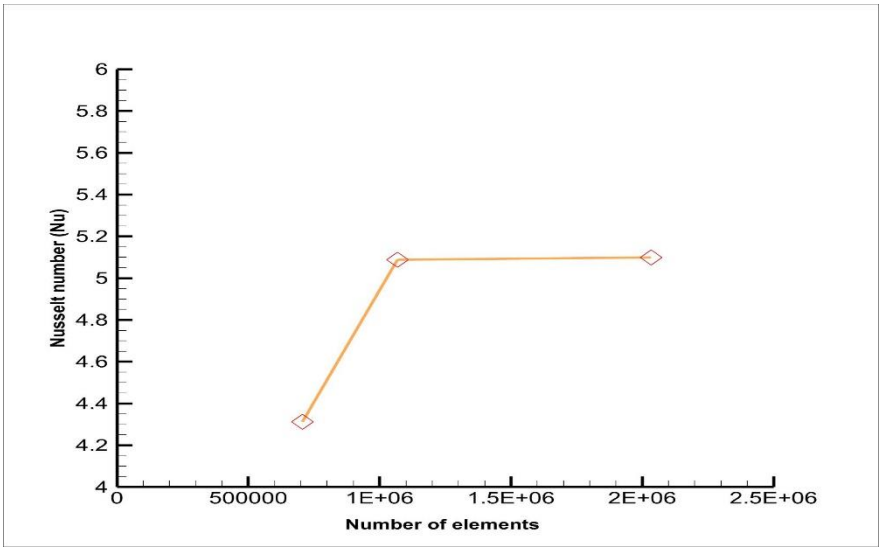

Figure 2.2Mesh Independence Test

3.5.3 Physics setup

As we know, implicit techniques have less time step constraints than explicit systems, they are favored for stable and slow transient flows. For stable incompressible flows, several solutions techniques utilize a pressure equation to ensure mass is conserved at each time step, often known as outer iteration for steady solvers.

SIMPLE is an abbreviation that stands for Semi-Implicit Method for Pressure Linked Equation. It is widely used as a numerical procedure to solve Navier –Stokes equation. Here, the velocity correction is solved explicitly, whereas implicit criteria of solving is used for the pressure correction and the discretized momentum equation. Hence it is termed as the "Semi-Implicit Method." Moreover, to solve the problem with a pressure based solver,second order discretization upwind is used. The various boundary conditions was incorporated along with the values generated from analytical calculation for rough microchannel, microchannel with sand grain roughness and smooth microchannel. In this study, the fluid considered is water and the material is steel.

3.5.4 Post processing and results

The results generated from the above will now be evaluated and all the run cases will be analyzed in order to understand the outputs of simulation. Since the research is focused on determining the effects of roughness on Nusselt number, every cases will be evaluated through the post-processing works using CFD tool.

After successful iteration, the post processing was done in order to calculate and validate the values with that obtained from numerical calculation.

As we know, Convective heat transfer at the wall is given by,

$$\ddot{q} = \frac{\mathrm{q}}{\mathrm{A}} = h\,(Twx - Tx) \tag{3.15}$$

where,

Twx= Local tube inside wall temperature

Tx= Local water temperature

Hence,

Nusselt number is given by,

$$\mathrm{Nu} = \frac{hL}{K} = \frac{\ddot{q} \times (2R)}{(Twx - Tx)} \tag{3.16}$$

The point cloud was created along the microchannel and then the maximum value of the temperature was calculated at that point. Then radial line was constructed to find out the mean temperature. Hence the local water temperature is defined as,

$$Tx = \frac{\int_0^R uT\,.\,dr}{\int_0^R u.dr} \tag{3.17}$$

3.6 Case Studies

3.6.1 Case Study 1: Smooth microchannel

Modeling of the geometry

The circular microchannel of mentioned values was constructed in ANSYS Design modeler in millimeters scale along with the sliced solid section as heated and unheated section and the fluid domain throughout the geometry.

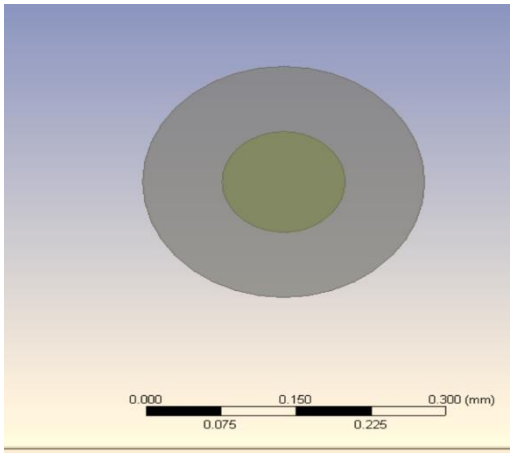

Figure 2.3Front view of the circular microchannel

Mesh generation

ANSYS Meshing 16 is used to import the geometry. Various type of meshing was tried and the best among them was choosen. The structured mesh with 282620 nodes and 222794 elements was created.

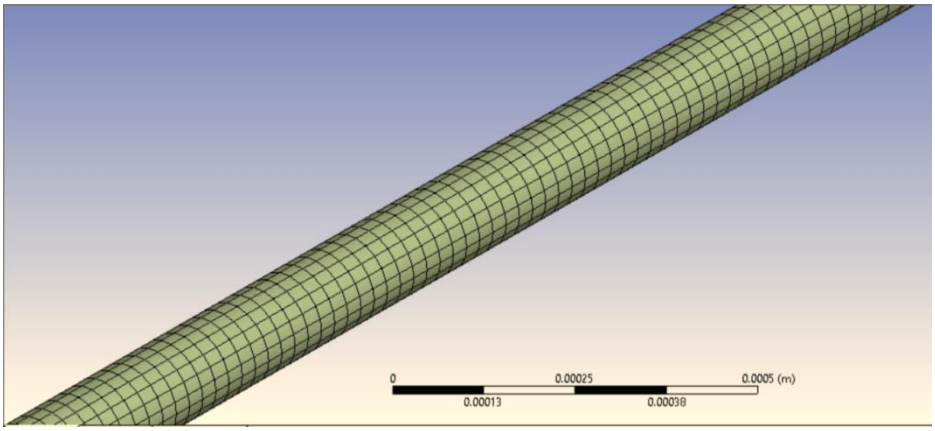

Figure 2.4Structured mesh (Isometric view)

Physics and boundary condition setup

The mesh is then loaded into ANSYS Fluent and the setup is complete. The fluid characteristics and type of turbulence model are selected during setup. In the ANSYS Meshing itself, the cell conditions are adjusted to fluid. After that, the setup is initialized, and the computation begins.

The physics was set up for smooth microchannel with Reynolds number of 424.4 with laminar flow.

At inlet side, velocity inlet was applied and the velocity of the flow was specified.

At outlet side, the specification of pressure outlet boundary condition was done where the average Static pressure was considered to be 0 [Pa].

At the wall, the constant heat flux was specified as calculated from numerical calculation.

3.6.2 Case Study 2: Microchannel with sand grain roughness

Modeling of the geometry

The circular microchannel of mentioned values was constructed in ANSYS Design modeler in millimeters scale along with the sliced solid section as heated and unheated section and the fluid domain throughout the geometry.

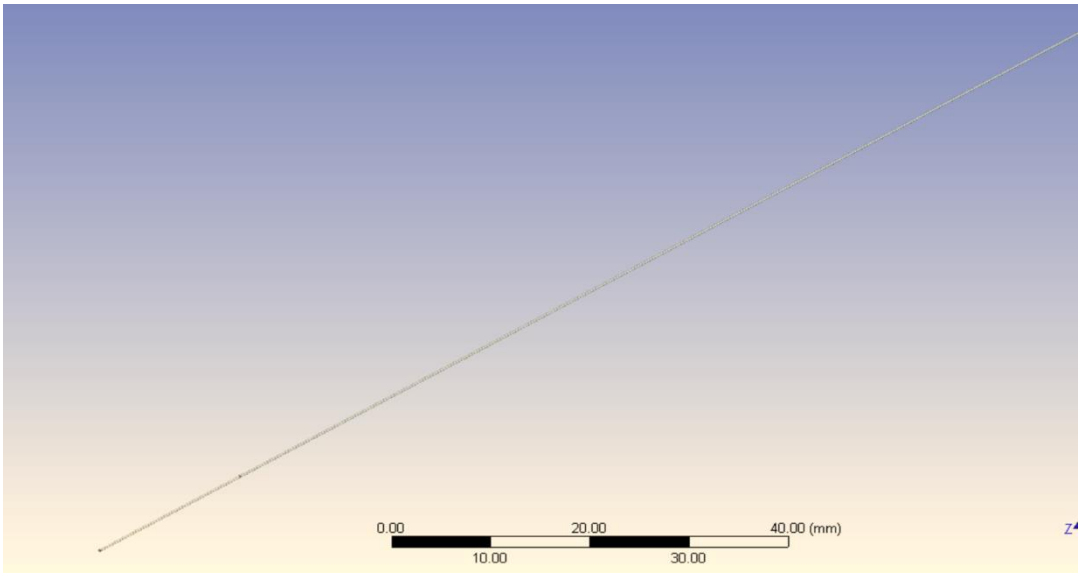

Figure 2.5 Full cross section of microchannel (Isometric View)

Mesh Generation

ANSYS Meshing 16 is used to import the geometry. Various type of meshing was tried and the better among them was chosen. The number of nodes and elements obtained were 195660 and 135850 respectively.

Physics and boundary condition setup

The surface roughness has a big impact on engineering issues and it causes more turbulence near rough walls. Additionally, it has an effect on raising wall shear stress. The ability to accurately estimate near-wall flows is dependent on a number of factors. Hence, Surface roughness should be properly modeled. In CFD analysis, surface roughness can be considered using special parameter known as sand grain roughness that depend on shape and frequency not only on roughness amplitude.

For rough walls, the logarithmic profile exists, but the near wall treatment becomes more complicated as we get closer to the wall, as it now depends on two variables: the

dimensionless wall distance y+ and the roughness height (Ra). The absolute roughness arithmetic average, which, like the wall border, must be provided.

Many commercial software packages provide this feature with the roughness equivalent to sand grains. It's crucial to remember that the roughness of the sand grain is significant. So the geometric roughness of the surface is not equal to the sand grain roughness height(Muhič & Mitruševski, 2017).

The mesh is loaded into ANSYS Fluent and the setup is complete. The fluid characteristics and turbulence model are selected during setup. In the ANSYS Meshing itself, the cell conditions are adjusted to fluid. After that, the setup is initialized, and the computation begins.

The physics was set up for smooth tube where the flow is turbulent with Reynolds number of 3000. In this κ-ε turbulence modeling is used with standard wall function. The traditional k- turbulence model is a two-equation model found in most commercial CFD programs (turbulence models in this context refers to dissipation). This model uses two transport equations to account for the turbulent characteristics of the flow to offer a broad description of turbulence.

The roughness height was kept as mentioned above along with the roughness constant of 0.5.

At inlet side, velocity inlet was applied and the velocity of the flow was specified.

At outlet side, pressure outlet boundary condition was specified.

At the wall, the constant heat flux was specified as calculated from numerical calculation.

3.6.3 Case Study 3: Single Regular Rough microchannel

Data Generation

Since in our study, the total tubes undertaken is fifteen and the average among them is taken as the main data for construction. Hence taking into account the standard deviation and average roughness, the data generation for internal, external and roughness was done and one of the value among them was choosen for constructing geometry and conducting the simulation in ANSYS. The data generation is attached in the appendix A.

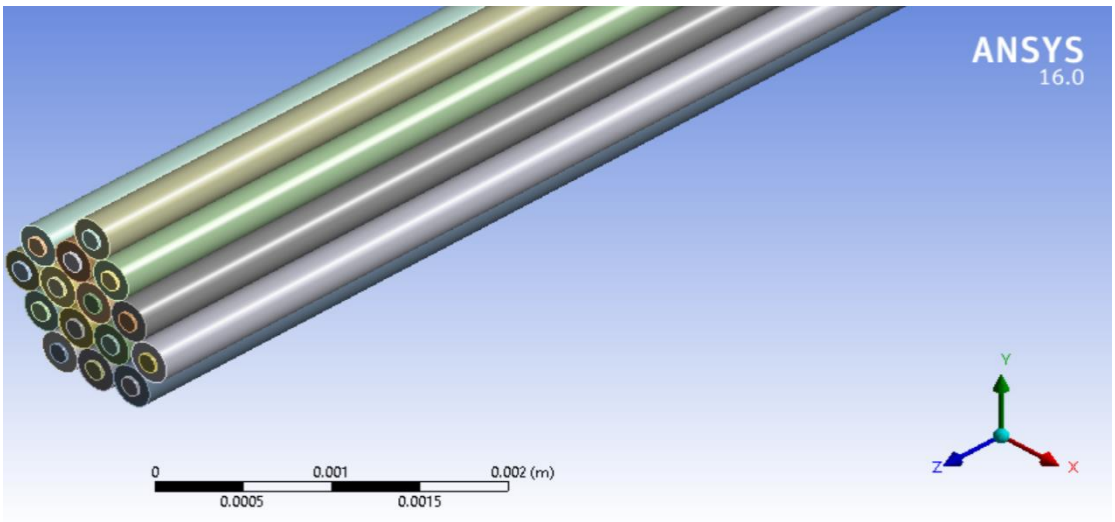

Figure 2.6Construction of fifteen microchannel in Solidworks

Modeling of the geometry

The circular microchannel of mentioned values was constructed in Solidworks in millimeters scale along with the regular roughness height of the surface as given. Then the model was exported to ANSYS Design modeler where the heated portion and fluid domain was defined.

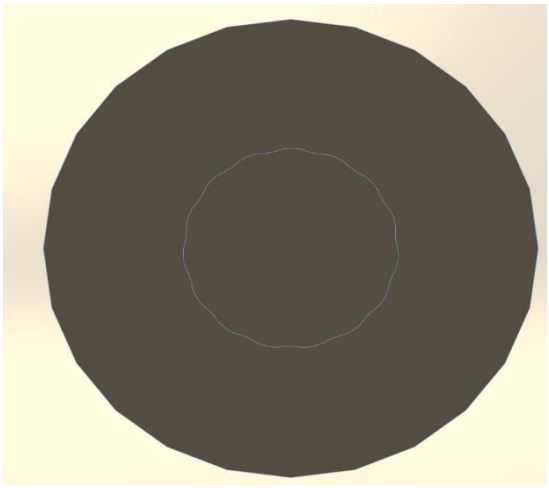

Figure 2.7 Regular Rough Tube

Mesh generation

ANSYS MESHING 16 is used to create mesh of geometry. Various type of meshing was tried and the better among them was choosen. The number of nodes and elements were 1148178 and 1067009 respectively.

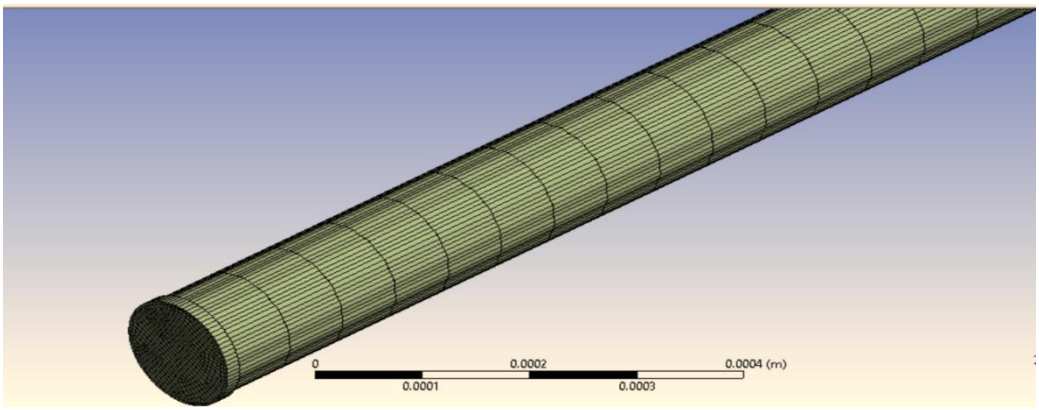

Figure 2.8 Mesh Generation of Rough microchannel

Physics and boundary condition setup

The mesh is then loaded into ANSYS Fluent and the setup is then continued. In the ANSYS Meshing itself, the cell conditions are adjusted to fluid. After that, the setup is initialized, and the computation begins.

The physics was set up for random rough microchannel where the flow is turbulent with Reynolds number of 2300.

In this κ-ε turbulence modeling is used with standard wall function. The traditional k-turbulence model is a two-equation model found in most commercial CFD programs (turbulence models in this context refers to dissipation). This model uses two transport equations to account for the turbulent characteristics of the flow to offer a broad description of turbulence. When there are no big adverse pressure gradients or strong local pressure shifts, this model operates well. In regions of re-attachment, turbulent kinetic energy can be over-predicted, resulting in poor prediction of the evolution of the boundary layer around bluff bodies and when separation occurs

At the inlet side, velocity inlet was applied and the velocity of the flow was specified.

At the outlet side, pressure outlet boundary condition was specified where the Average Static Pressure was considered to be 0 [Pa].

At the wall, the constant heat flux was specified as calculated from numerical calculation.

3.6.4Case Study 4: Random rough microchannel

Surface roughness study

Roughness modeling is done by spatial frequency method. A Gaussian Distribution Surface is used to generate 3D surface roughness.

The Fourier series expansion based on the sum of trigonometric functions, is analogous to describing surface roughness using spatial frequency method. Each term used represents a certain frequency of oscillation.

Rough surface z(x,y) is represented as collection of numerous elementary waves, where Φ is phase angle. The phase angle is important for creating a random surface with an elementary wave. The value is choosen using Gaussian distribution, allowing the equation cos (Φ) to encompass all values between -1 and +1.The dynamics of the created rough surface created as the summation of all wave components is governed by the equation:

$$z(x,y) = \sum_{m=-M}^{M} \sum_{n=-N}^{N} A_{mn}\, Cos(2\pi(mx + ny) + \Phi_{mn})$$

where,

$$A_{mn} = w(m,n) = \frac{1}{(m^2 + n^2)^{\frac{\beta}{2}}}$$

represents the Amplitude of the random Gaussian distribution. Phase angle is varied between (-$\frac{\pi}{2}$, $\frac{\pi}{2}$) and the associated rough surface profile is created. 'm' and 'n' represent spatial frequencies along the abscissa and ordinate respectively.

Data generation

The construction of random cylinder is to be done by the data generation in three dimensions through MATLAB coding. The data is created and then converted to Cartesian coordinates which is to be imported to Solidworks for surface and geometry generation. After geometry construction, it will be further transported to ANSYS for further meshing and simulation.

CHAPTER FOUR: RESULTS AND DISCUSSION

In accordance to the methodology written above, the data collection was done which was then followed by the construction of geometry in ANSYS Design modeler and Solid works as per the case. The setup was done in ANSYS Fluent software. After successful iteration, the post processing was done in order to calculate and validate the values with that obtained from numerical calculation.

4.1 Results from simulation

4.1.1 Smooth microchannel

The simulation is conducted in ANSYS fluent. One of the most important requirements is to ensure that a sufficient number of iterations have been completed that is done in order to get the desired outcome. While executing the procedure, parameters can be monitored. In this case, the solution was converged run with 1000 iterations. After successful iteration, the post processing was done in order to calculate and validate the values with that obtained from numerical calculation. The value for Nusselt number was obtained as 4.059 that deviated from the value obtained from the numerical correlation of Nusselt number.

4.1.2 Microchannel with sand grain roughness

The simulation is conducted in ANSYS Fluent. One of the most important requirements is to ensure that a sufficient number of iterations have been completed that is done in order to get the desired outcome. The physics was setup as described above and after successful iteration. The value of Nusselt number for this case was obtained was 4.13466 that deviated from the value obtained from correlation defined earlier.

4.1.3 Single regular rough microchannel

The simulation here is also conducted in ANSYS Fluent after importing the geometry from Solidworks. One of the most important requirements is to ensure that a sufficient number of iterations have been completed that is done in order to get the desired outcome. While executing the procedure, parameters can be monitored. After successful iteration, the post processing was done in order to calculate and validate the values with that obtained from numerical calculation. The value of Nusselt number was found to be 5.08856.

4.1.4 Random rough microchannel

MATLAB programming was done to generate and study the nature of surface roughness. The spatial frequency are denoted as M and N and the size of the surface in two dimensions in order to generate a surface. Furthermore, with the availability of hydraulic diameter of the channel as well as the intended relative roughness, the created surface is modified to incorporate the required roughness value.

For sake of understanding, parameters M, N, and β are varied and the corresponding change in the roughness profile is observed.

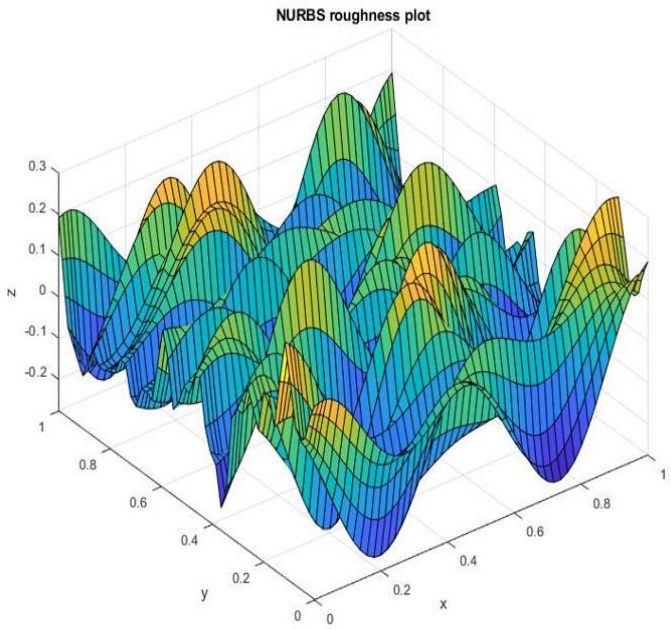

Figure 3.1Roughness Profile for M=2, N=16, β =0.5

Figure 4.1 and Figure 4.2 represent the change in the nature of the roughness for changing the value of β for M=16, N=16. It is observed that the higher value of β results in the smooth surface profile meaning that it acts as a damping force to attenuate the amplitude of the peaks. The lower the value of β goes, the amplitude of the peaks are increased, resulting in more irregular surface.

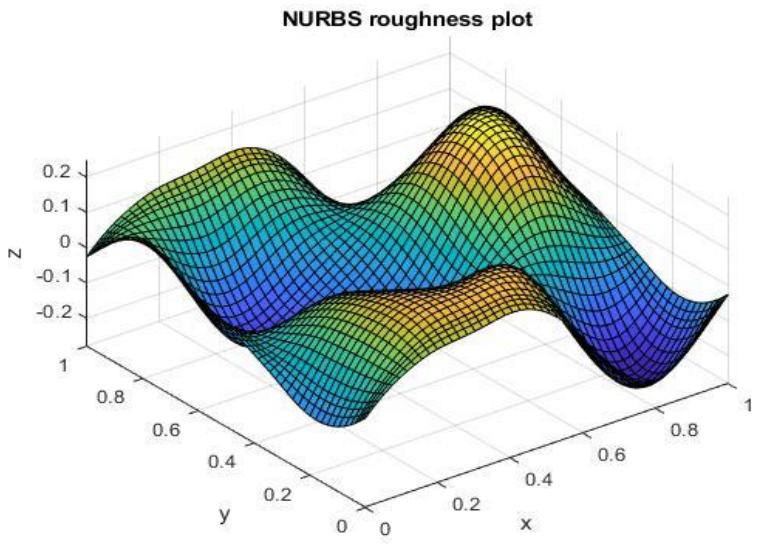

Figure 3.2 Roughness Profile for M=16, N=16, β =5

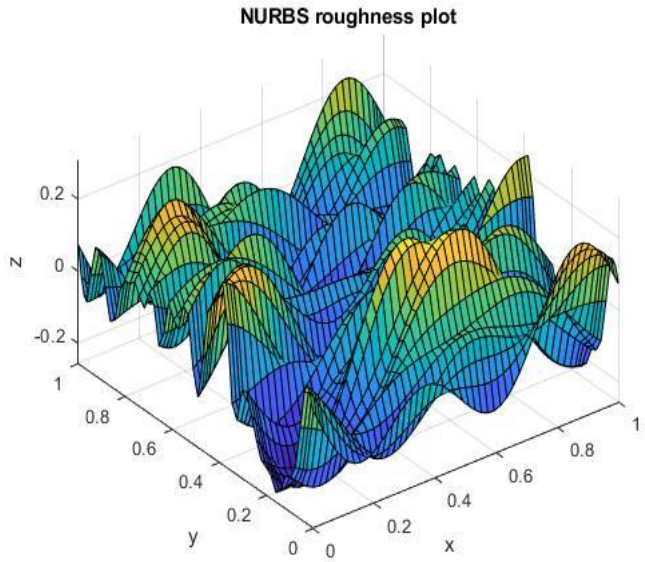

Figure 3.3 Roughness Profile for M=16, N=16, β =1

Figure 4.3 and Figure 4.4 represent the roughness profile for varying M keeping the other two parameters, i.e. N and β constant. It is observed that the high value of M results in a lower wavelength of the surface profile along the abscissa. Also, reduction in the value of M results in fewer waves along the aforementioned direction. Similar is the case with varying N, keeping the other two parameters constant, wherein the change in N has control over the number of waves along the ordinates, as shown in figure 4.5 and figure 4.6.

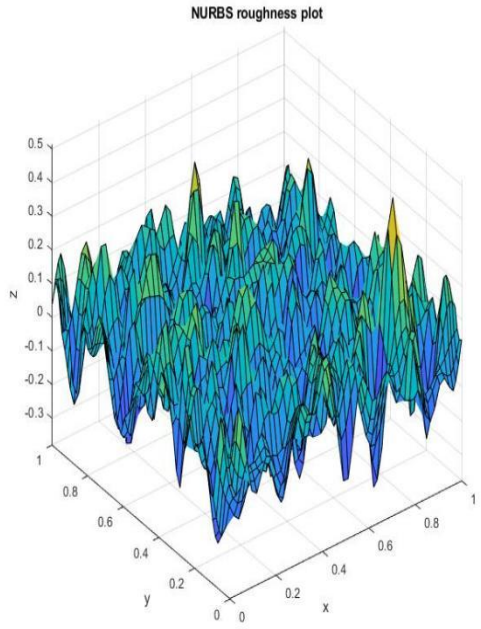

Figure 3.4 Roughness Profile for M=10, N=16, β =0.5

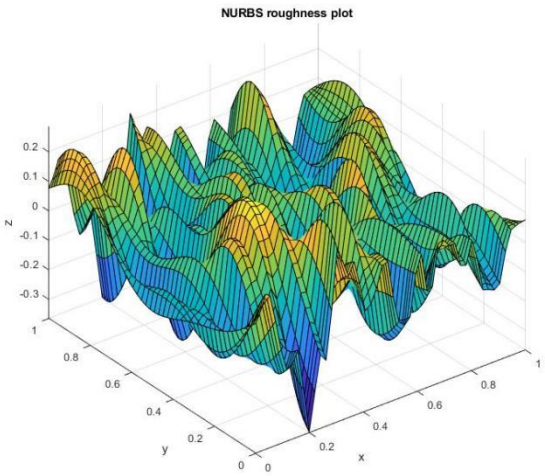

Figure 3.5 Roughness Profile for M=16, N=2, β =0.5

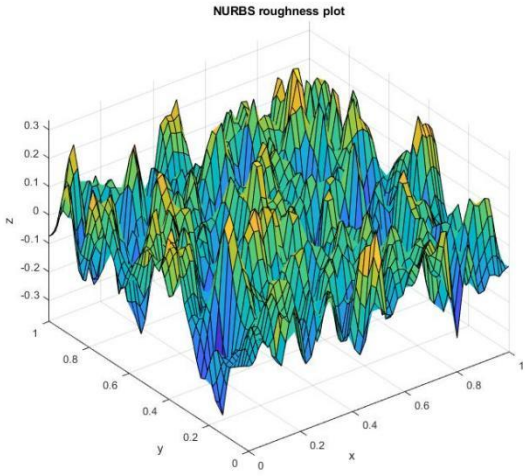

Figure 3.6 Roughness Profile for M=16, N=10, β =0.5

So, by varying the parameters M, N, and b, the surface profile can be varied. The degree of randomness can be controlled by varying the parameters in the defined Gaussian distribution function. The parameters M, N, and b can be tuned until the desired roughness is achieved. The statistical parameters such as Skewness, Kurtosis of the randomly distributed profile can be calculated as per the requirement. The MATLAB code to achieve the plot from figure is attached in the annex B.

3D cylindrical surface of length 50 mm is created in MATLAB. A random function for the radius of the cylindrical is taken to have an irregular surface of the cylinder. The radius of the cylinder is varied within 1-5 % of 123 mm. The idea is to have different radii along the length of the cylinder, with the rotation axis being kept between 0 to 2π. The plot obtained from the MATLAB is shown in figures below respectively. The MATLAB code to obtain the plot is attached in Annex B. The obtained surface from the MATLAB is to be exported to ANSYS and used to model 3D.

In the figures below, the cross sectional area and cylindrical plot is generated for 5 cases of percentage ranging from 1-5%. We can see as the percentage of roughness increases it appears to be more random and then we take this as our reference for study.

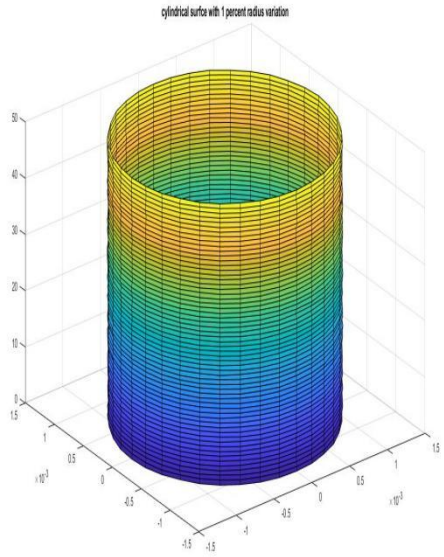

Figure 3.7 3D Cylindrical Surface with 1 % radius variation

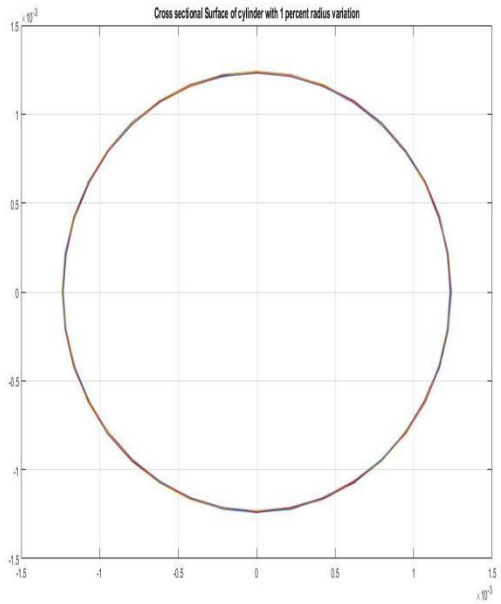

Figure 3.8 Cross Sectional Area of Cylindrical surface for 1 % radius Variation

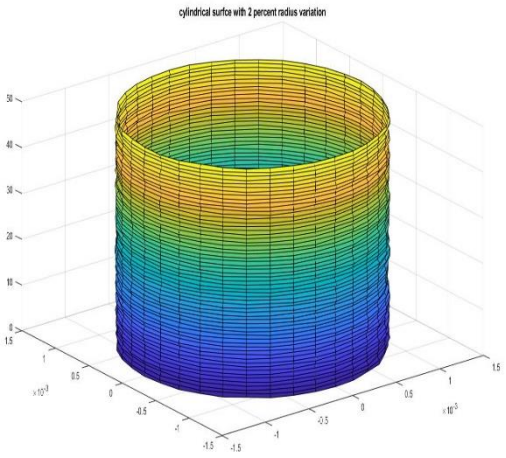

Figure 3.9 3D Cylindrical Surface with 2 % radius variation

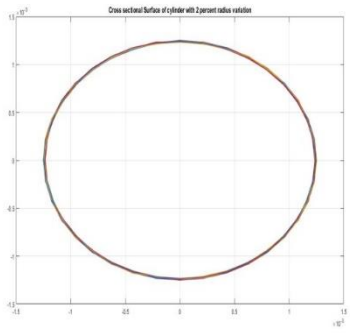

Figure 3.10 Cross sectional area of cylindrical Surface for 2 % radius variation

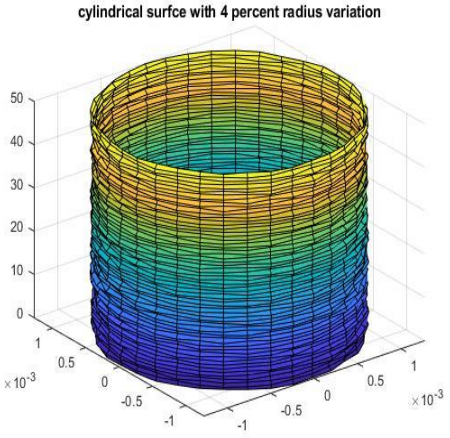

Figure 3.11 3D Cylindrical surface with 3 % radius variation

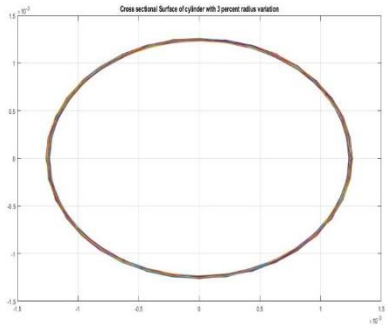

Figure 3.12 Cross sectional area of cylindrical Surface for 3 % radius variation

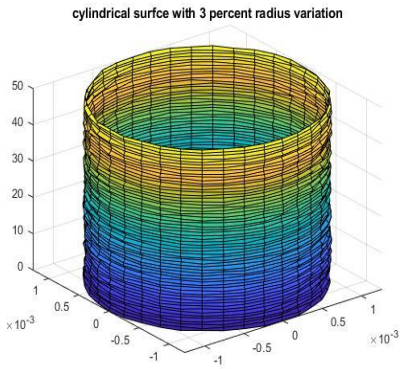

Figure 3.13 3D Cylindrical surface with 4 % radius variation

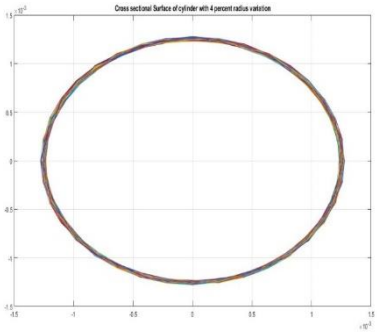

Figure 3.14 Cross sectional area of cylindrical surface for 4 % radius variation

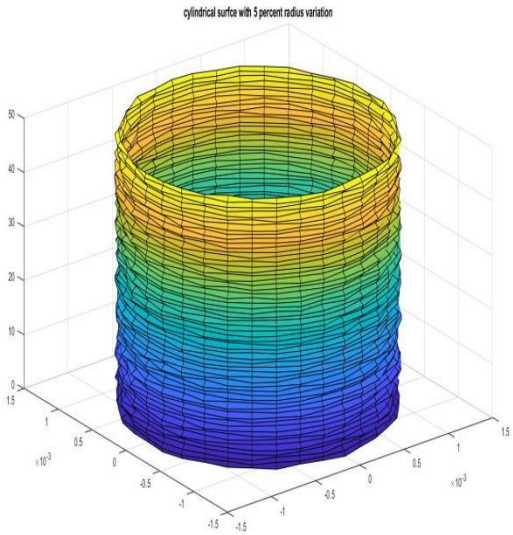

Figure 3.15 3D Cylindrical surface with 5 % radius variation

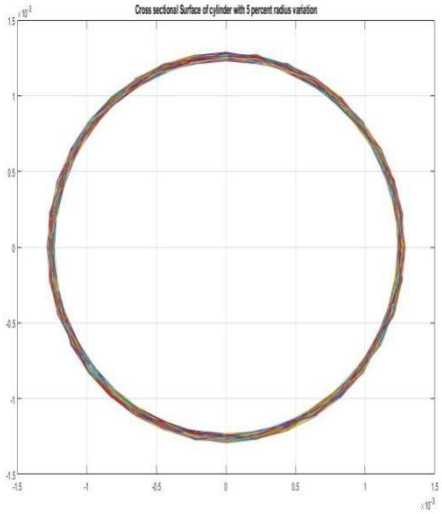

Figure 3.16 Cross sectional area of cylindrical Surface for 5 % radius variation

The data with roughness 5% was chosen and then it was exported to Solid works. But since the dimension is small, results couldn't be derived properly. So similitude condition has been used.

Similitude refers to the similarity between a prototype and its model. It implies that the model and prototype will have comparable features, or that similitude indicates that the model and prototype will be identical. It is used for the fluid flow conditions with scaled models. For perfect similitude between a model and its prototype, certain types of similarities like kinetic, geometric and dynamic similarity must exist. So the prepared modeled is scaled up as shown in figure below and then the simulation was continued thereafter.

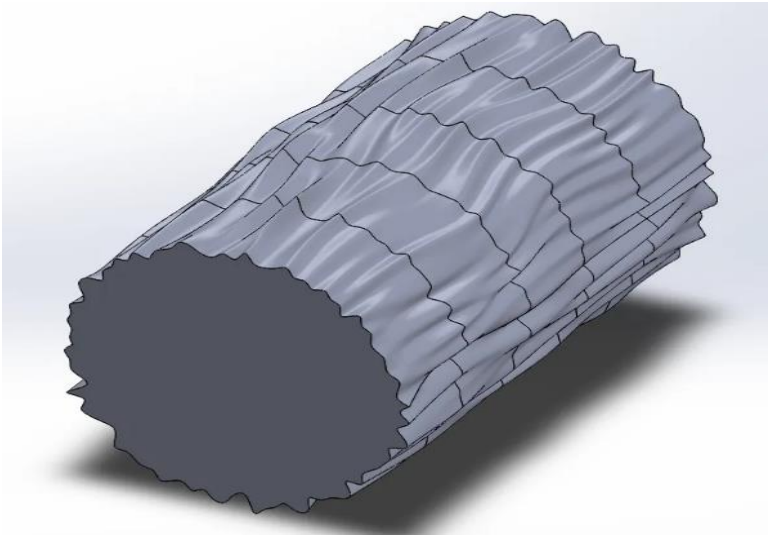

Figure 3.17 3D rough microchannel

After the geometry is imported, the mesh is then loaded into ANSYS Fluent and the setup is complete. The fluid characteristics and turbulence model are selected during setup. After that, the setup is initialized, and the computation begins.

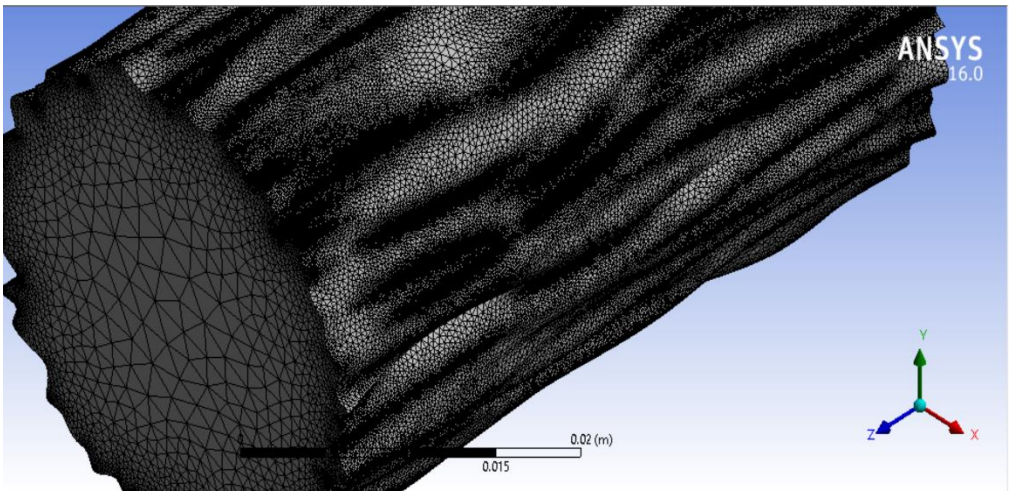

Figure 3.18 Meshing of the rough microchannel

The physics was set up where the flow is turbulent with Reynolds number of 3000.

At inlet side, velocity inlet was applied and the velocity of the flow was specified.

At outlet side, pressure outlet boundary condition was specified.

At the wall, the constant heat flux was specified as calculated from numerical calculation.

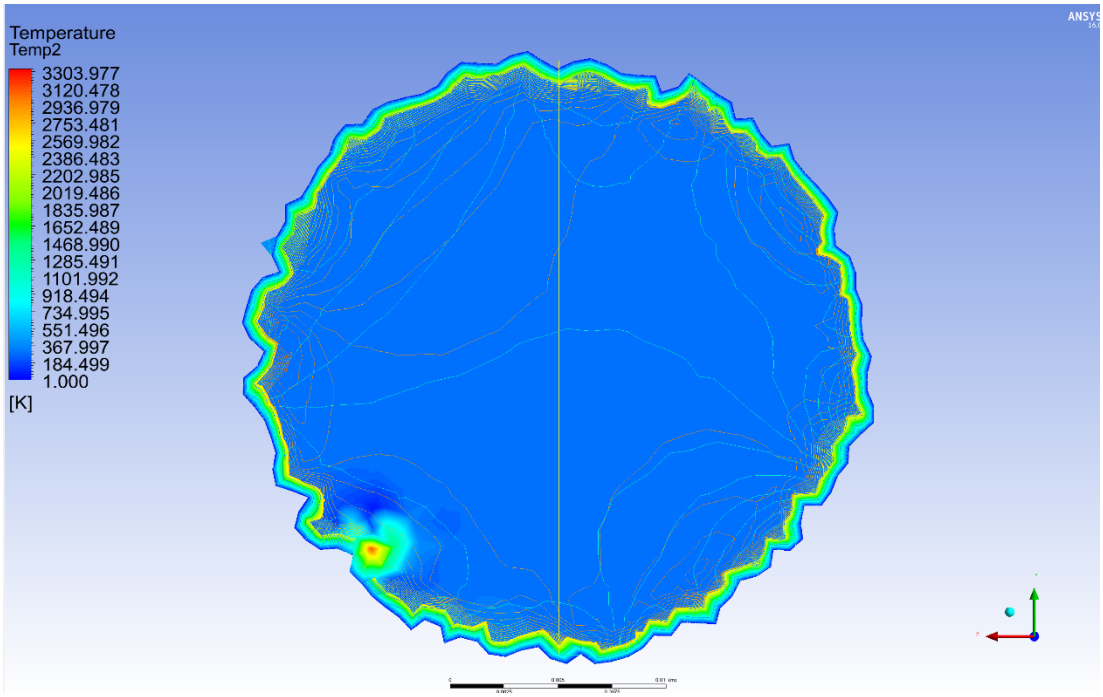

Figure 3.19 Temperature contour at inlet side

We can see from the above figure that the temperature near the wall is maximum and since the boundary condition is provided as constant heat flux the temperature is constant in that area.

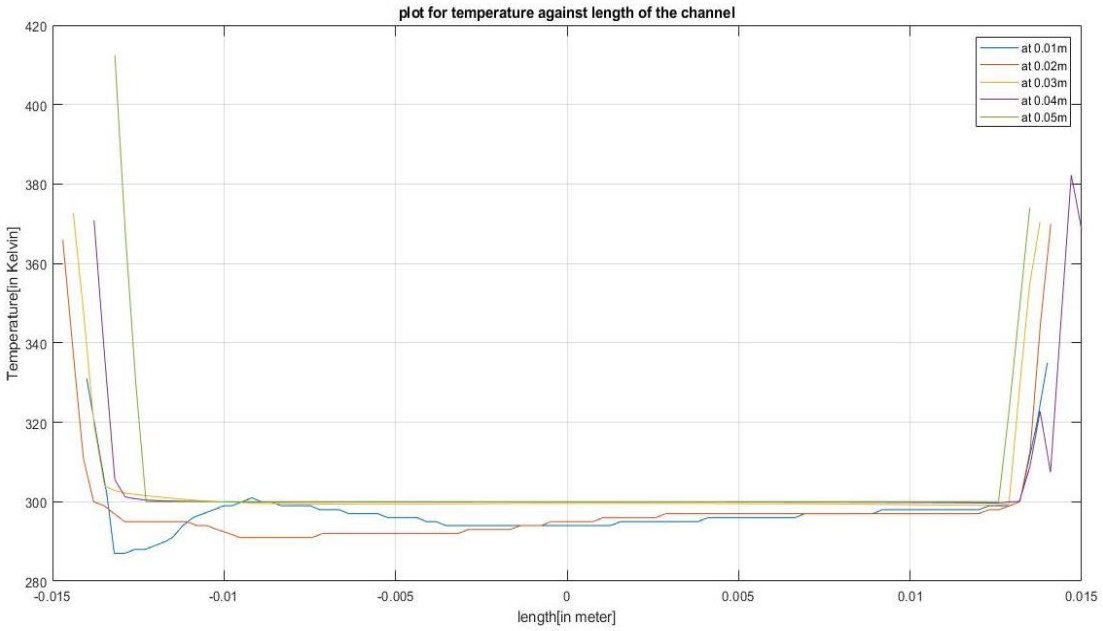

Figure 3.20 Temperature vs length along the channel for five locations

The temperature was checked at various locations throughout the axial length of the channel and the data were plotted and we see the graph of temperature and length as shown.

Then the contour for velocity was also developed. We can see that wall velocity is zero while at inlet we can see the velocity remained almost constant. Same conclusion can be drawn from the velocity contour developed along the length in the figure below.

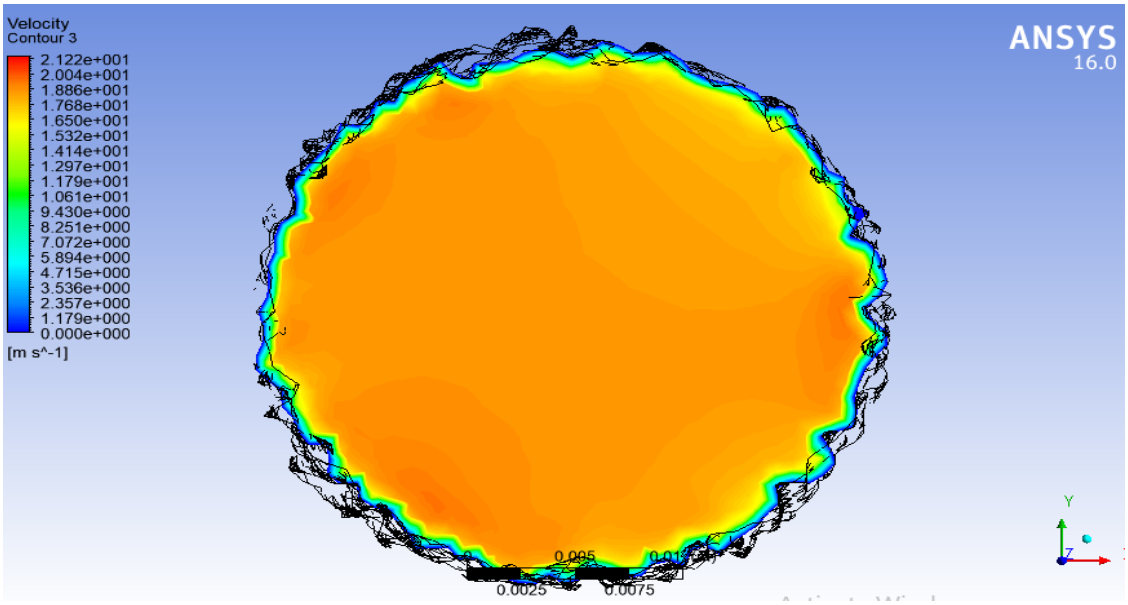

Figure 3.21 Velocity contour at the inlet side of the channel

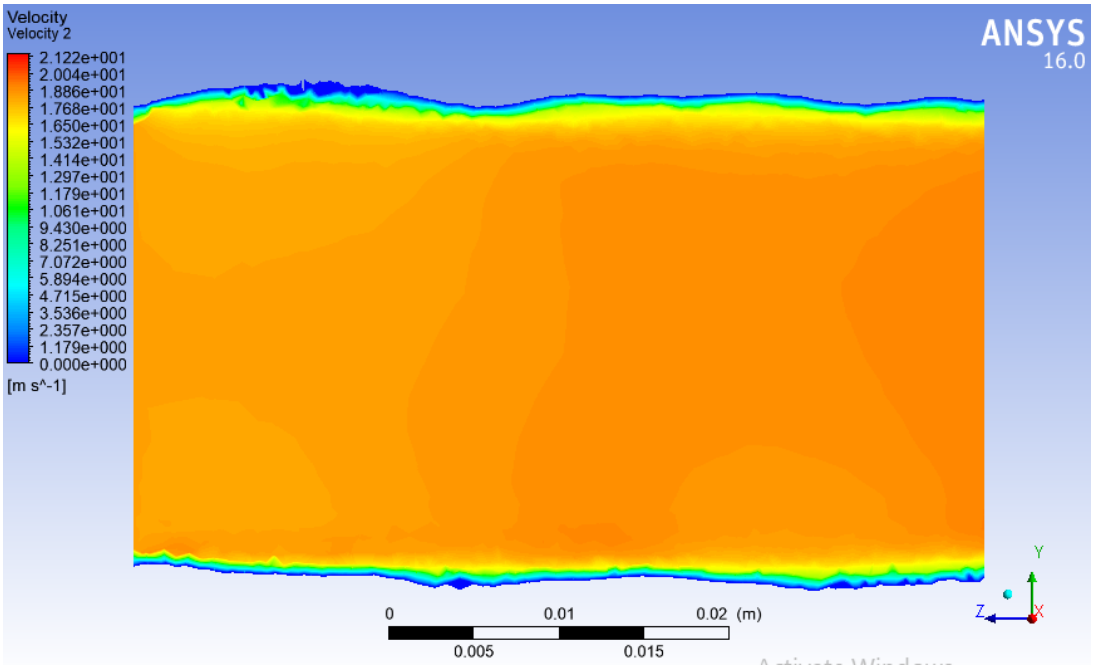

Figure 3.22 Velocity contour along the axial length of the channel

4.2 Performance parameters

The performance parameters of various types of microchannel has been enlisted below along with the comparison with the values derived from analytical calculation and software simulation.

Table 3.1 Summary of values

SN	Microchannel Type	Value from simulation	Value from analytical calculation	Percentage Error
1	Smooth	4.059	4.36412	7.5%
2	Channel with sand grain roughness	4.13466	3.8129	8.4%
3	Regular rough channel	5.08856	5.4355	6.817%

From above all, it can be justified that the microchannel created with the randomly generated profile holds better value than the other case. This justifies the real case scenario in the construction of microchannel by various micromachining techniques where are surface deviation will be seen.

For the regular rough microchannel, the data was obtained for the Nusselt number for range of Reynolds through simulation. The dynamics of the relationship between the Nusselt number and the Reynold number were captured using the Polynomial Curve fitting method. The curve obtained from MATLAB is shown in the figure 4.23.

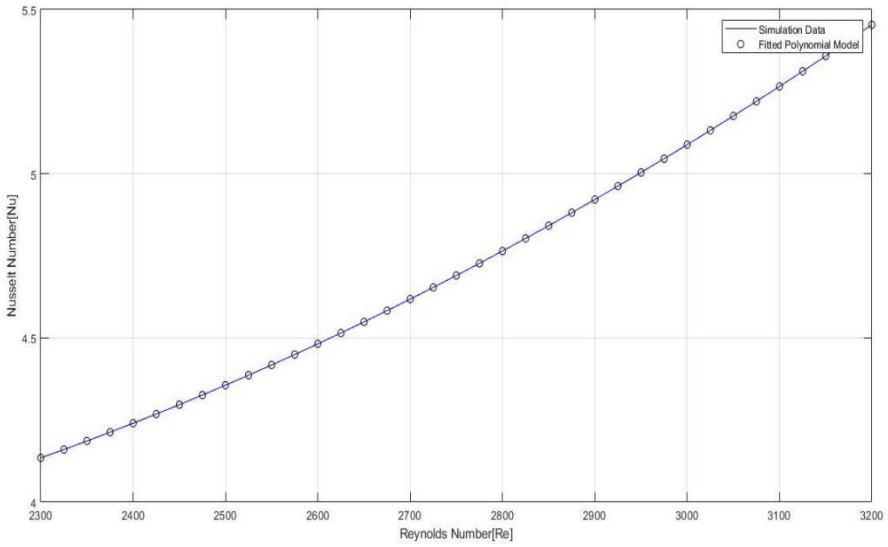

Figure 3.23 Graph showing Nu vs Re with simulation data and polynomial model

The simulated data were plotted against the fitted polynomial model, representing the simulated data. The order of the polynomial was varied and the polynomial of order 2 was observed to be enough to represent the simulated data. The simulated data was calculated to be governed by the obtained polynomial equation of order 2 as:

$$p(x) = 5.134 \times 10^{-7} \times x^2 - 1.3584 \times 10^{-3} \times x + 4.543$$

Where x represents the Reynold Number and p(x) represents the corresponding Nusselt Number.

The root means square error for the fitted data against the data obtained from the simulation was calculated to be in the order of 10^{-14}. The error plot for the difference between values obtained from the fitted polynomial curve and from the simulation, for the same Reynold Number is shown in the figure.

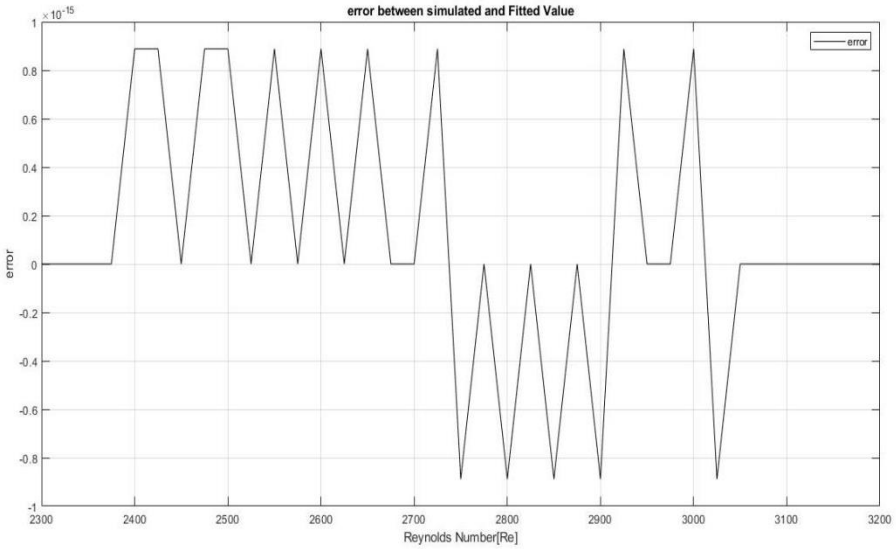

Figure 3.24 Graph showing error between simulated and Fitted value

The error plot shows the negligible difference between the data obtained from the fitted model and simulated data, which suggests the aforementioned polynomial is the best fit for system under consideration.

Similarly, the Nusselt number for regular rough microchannel was calculated analytically using equation 3.10 for varying Reynold numbers from 2300-3200. The data obtained from the calculation was plotted against the Reynold Number. The plot representing the data obtained from the analytical calculation and through the simulation is shown in the figure.

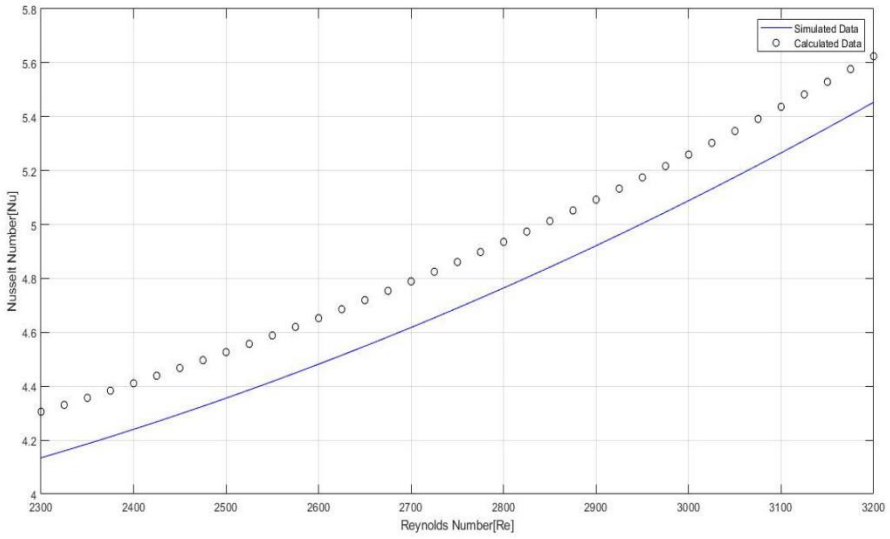

Figure 3.25 Graph of Nu vs Re of calculated and simulated data

The root means the square error was used as a performance parameter to assess the difference between the data obtained from the simulation and the data obtained from the analytical calculation. The root means square error for the difference between the aforementioned data was calculated to be 17.08 %. The error plot showing the difference between the analytical output and the simulated output is shown in the figure. And the MATLAB code to obtain the plot from figure 4.23 to figure 4.26 is attached in the appendix B.

CHAPTER FIVE: CONCLUSIONS AND RECOMMENDATIONS

5.1 Conclusions

Following conclusions have been drawn from the study

- The study of roughness was done by modeling through spatial frequency method where the Gaussian distribution was used to generate 3D surface roughness. The programming was done in MATLAB and the variations has been done in parameters like spatial frequency and spectral exponent which controlled the degree of randomness.
- In order to generate a random cylinder, variation has been done within 1-5 % of internal diameter. And it has been found that keeping the value of roughness percentage greater yielded a realistic image of manufacturing than the one with the smooth finishing.
- Out of two method used for roughness modelling, it was found that random rough modelling yielded a realistic image of manufacturing than the one with the regular rough modeling.
- Summarizing from all the cases, the value of Nusselt number achieved from numerical simulations almost have been similar to that obtained from analytical calculations with an average error of 7.5% for three cases studied.

5.2 Recommendations

To improve the microchannel design approach in future research, the recommendations for continuing this work have been summarized in the points below.

- In order to evaluate and minimize the consequent inequalities in the reported results, thorough investigations with appropriate design, fabrication, and instrumentation of the microchannels are required.
- Although only heat transfer characteristics is studied in this research for performance analysis, other parameters can be studied in order to recognize the outcome on the performance as well as effects of roughness on them.
- Further with the availability of micro machining techniques, experimental study is recommended for validation and improvement of research.

REFERENCES

Adams, T., & Grant, C. (2012). A Simple Algorithm to Relate Measured Surface Roughness to Equivalent Sand-grain Roughness. 1(1). https://doi.org/10.11159/ijmem.2012.008

Adams, T. M., Jeter, S. M., & Qureshis, Z. H. (1997). An experimental investigation of single-phase forced convection in microchannels. 41, 851–857.

Ameel, T. A., Warrington, R. O., Wegeng, R. S., & Drost, M. K. (1997). Miniaturization technologies applied to energy systems. Energy Conversion and Management, 38(10–13), 969–982. https://doi.org/10.1016/s0196-8904(96)00127-6

Celata, G. P., & Cumo, M. L. (2003). Water Single-Phase Fluid Flow and Heat Transfer in Capillary Tubes. June 2014. https://doi.org/10.1115/ICMM2003-1037

Celata, G. P., Cumo, M., & Zummo, G. (2004). Thermal-hydraulic characteristics of single-phase flow in capillary pipes. Experimental Thermal and Fluid Science, 28(2–3), 87–95. https://doi.org/10.1016/S0894-1777(03)00026-8

Dongqing, L., & Mala, G. M. (1999). Flow characteristics of water in microtubes. Chinese Physics Letters, 23(12), 3305–3308. https://doi.org/10.1088/0256-307X/23/12/051

Fung, C. K., & Majnis, M. F. (2019). Computational fluid dynamic simulation analysis of effect of microchannel geometry on thermal and hydraulic performances of micro channel heat exchanger. Journal of Advanced Research in Fluid Mechanics and Thermal Sciences, 62(2), 198–208.

Gad-el-Hak, M., & Seemann, W. (2002). MEMS Handbook. In Applied Mechanics Reviews (Vol. 55, Issue 6). CRC PRESS. https://doi.org/10.1115/1.1508147

Guo, L., Xu, H., & Gong, L. (2015). Influence of wall roughness models on fluid flow and heat transfer in microchannels. Applied Thermal Engineering, 84, 399–408. https://doi.org/10.1016/j.applthermaleng.2015.04.001

Hasan, M. I., Hasan, H. M., & Abid, G. A. (2014). Study of the axial heat conduction in parallel flow microchannel heat exchanger. Journal of King Saud University - Engineering Sciences, 26(2), 122–131. https://doi.org/10.1016/j.jksues.2012.12.004

Hetsroni, G., Mosyak, A., Pogrebnyak, E., & Yarin, L. P. (2011). Micro-channels: Reality and myth. Journal of Fluids Engineering, Transactions of the ASME, 133(12). https://doi.org/10.1115/1.4005317

Kandlikar, S. G. (2008). Exploring roughness effect on laminar internal flow-are we ready for change? Nanoscale and Microscale Thermophysical Engineering, 12(1), 61–82. https://doi.org/10.1080/15567260701866728

Khan, M. N., Islam, M., & Hasan, M. M. (2010). Alternative Approach for predicting Average Nusselt Number for Fully Developed Flow in Circular Microchannels. Channels, 2(8), 3557–3560.

Koo, J., & Kleinstreuer, C. (2005). Analysis of surface roughness effects on heat transfer in micro-conduits. International Journal of Heat and Mass Transfer,

48(13), 2625–2634. https://doi.org/10.1016/j.ijheatmasstransfer.2005.01.024

Krishnamoorthy, C., & Ghajar, A. (2014). Single-Phase Heat Transfer in Micro-Tubes : A Critical Review HT2007-32408. April. https://doi.org/10.1115/HT2007-32408

Lelea, D., Nishio, S., & Takano, K. (2004). The experimental research on microtube heat transfer and fluid flow of distilled water. International Journal of Heat and Mass Transfer, 47(12–13), 2817–2830. https://doi.org/10.1016/j.ijheatmasstransfer.2003.11.034

Lin, T. Y., & Yang, C. Y. (2007). An experimental investigation on forced convection heat transfer performance in micro tubes by the method of liquid crystal thermography. International Journal of Heat and Mass Transfer, 50(23–24), 4736–4742. https://doi.org/10.1016/j.ijheatmasstransfer.2007.03.038

Liu, Y., Xu, G., Sun, J., & Li, H. (2015). Investigation of the roughness effect on flow behavior and heat transfer characteristics in microchannels. International Journal of Heat and Mass Transfer, 83, 11–20. https://doi.org/10.1016/j.ijheatmasstransfer.2014.11.060

Lu, H., Duan, X., Xu, M., Gong, L., & Ding, B. (2020). A new method of roughness construction and analysis of construct parameters. CMES - Computer Modeling in Engineering and Sciences, 123(3), 1193–1204. https://doi.org/10.32604/cmes.2020.08989

Muhič, A., & Mitruševski, S. (2017). Wall Roughness Influence on the Efficiency Characteristics of Centrifugal Pump. 63, 529–536. https://doi.org/10.5545/sv-jme.2017.4526

Peiyi, W., & Little, W. A. (1983). Measurement of friction factors for the flow of gases in very fine channels used for microminiature Joule-Thomson refrigerators. Cryogenics, 23(5), 273–277. https://doi.org/10.1016/0011-2275(83)90150-9

Sobhan, C. B., & Garimella, S. V. (2001). A comparative analysis of studies on heat transfer and fluid flow in microchannels. Microscale Thermophysical Engineering, 5(4), 293–311. https://doi.org/10.1080/10893950152646759

Swift, G., Migliori, A., & Wheatley, J. (1985). Construction of and measurements with an extremely compact cross-flow heat exchanger. Heat Transfer Engineering, 6(2), 39–47. https://doi.org/10.1080/01457638508939623

Tuckerman, D. B., & Pease, R. F. W. (2013). High-Performance Heat Sinking for VLSI. November. https://doi.org/10.1109/EDL.1981.25367

Xing, Y., Zhi, T., Haiwang, L., & Yitu, T. (2016). Experimental investigation of surface roughness effects on flow behavior and heat transfer characteristics for circular microchannels. Chinese Journal of Aeronautics, 4–10. https://doi.org/10.1016/j.cja.2016.10.006

Yang, C., & Lin, T. (2007). Heat transfer characteristics of water flow in microtubes. 32, 432–439. https://doi.org/10.1016/j.expthermflusci.2007.05.006

Yang, C. Y., Chen, C. W., Lin, T. Y., & Kandlikar, S. G. (2012). Heat transfer and friction characteristics of air flow in microtubes. Experimental Thermal and Fluid Science, 37, 12–18. https://doi.org/10.1016/j.expthermflusci.2011.09.003

APPENDIX A: DATA GENERATION OF ROUGH CHANNEL

Mean=123 micro mm

SD= 3 micro mm

Table 1-A Data Generation for Internal Diameter

S.N.	Value	X=Value- Mean	X^2
1.	121.68	-1.288299634	1.659715946
2	121.82	-1.150331383	1.323262291
3	121.68	-1.284551182	1.650071738
4	122.92	-0.049699844	0.002470074
5	123.54	0.566760894	0.321217911
6	123.17	0.197292726	0.03892442
7	124.88	1.912762944	3.65866208
8	121.55	-1.423040002	2.025042846
9	122.15	-0.822744337	0.676908245
10	120.32	-2.653806976	7.042691467
11	122.24	-0.727236322	0.528872668
12	124.58	1.613162454	2.602293103
13	125.40	2.432612986	5.917605942
14	123.90	0.932659655	0.869854032
15	124.71	1.744458021	3.043133785
Mean	122.97		31.36072655
			2.090715103
		SD calculated	1.445930532

Mean=282 micro mm

SD= 3 micro mm

Table 1-B Data Generation for External Diameter

S.N.	Value	X=Value- Mean	X^2
1	279.63	-3.368212679	11.34485665
2	288.10	5.101472359	26.02502023
3	282.88	-0.122468373	0.014998502
4	281.80	-1.195562999	1.429370884
5	281.11	-1.894468883	3.589012349
6	280.72	-2.278576565	5.191911161
7	284.55	1.547588876	2.39503133
8	279.03	-3.967980368	15.7448682
9	285.91	2.911126298	8.474656322
10	276.72	-6.284198335	39.49114871
11	283.50	0.499212184	0.249212805
12	284.99	1.994367702	3.977502529
13	287.21	4.215348002	17.76915878
14	283.93	0.928491249	0.862096
15	284.91	1.913861531	3.662865959
Mean	282.9995272		140.2217104
			9.348114028
		SD calculated	3.057468565

Mean=1.4 micro mm

SD =0.3 micro mm

Table 1-C: Data Generation for Roughness

S.N.	Value	X= Value-Mean	X^2
1	1.127904631	-0.252191677	0.063600642
2	1.462827624	0.082731316	0.006844471
3	1.656328154	0.276231846	0.076304033
4	1.222420578	-0.15767573	0.024861636
5	1.711862253	0.331765945	0.110068642
6	1.458080821	0.077984513	0.006081584
7	1.523092311	0.142996003	0.020447857
8	1.33039252	-0.049703788	0.002470467
9	1.467468888	0.08737258	0.007633968
10	1.370138476	-0.009957832	9.91584E-05
11	1.317414247	-0.062682061	0.003929041
12	0.612193982	-0.767902326	0.589673982
13	1.625665411	0.245569103	0.060304184
14	1.288668257	-0.091428051	0.008359089
15	1.526986468	0.14689016	0.021576719
Mean	1.380096308		1.002255472
			0.066817031
		SD calculated	0.258489906

APPENDIX B: MATLAB CODES

i) MATLAB code to create the irregular surface

a)

```
clc
clear all
close all
format bank
format compact
d = 500; %diameter
r_scale = 250; % scaling ratio
r = 5.0; %roughness value that is desirable
MF=16; NF=10; b=0.5;
xa=0:0.02:1;
% tht = linspace(0,2*pi,1);
% x=repmat(61.56*cos(tht),51,1);
% y=repmat(61.56*sin(tht),51,1);
ya=0:0.02:1;
g1 = randn(2*MF+1,2*NF+1);
h = @(m,n) 0.05/((m^2+n^2)^(b/2));
phil =rand(2*MF+1,2*NF+1)*5;
mean_angle = mean(mean(phil));
phi_diff = phil- mean_angle;
u = phi_diff * pi;
n1 = length(xa); n2 = length(ya);
g_initial = zeros(n1,n2);
for l=-MF:1:MF
for k=-NF:1:NF
if l~=0 && k~=0
for v=1:n1
for w=1:n2
g_initial(v,w)=g_initial(v,w)+h(l,k).*g1(l+MF+1,k+NF+1).*cos(2*pi*(l*xa(v)+k*ya(
w))+u(l+MF+1,k+NF+1)); %Periodicity of the signal
end
end
end
end
end
[X,Y] = meshgrid(xa,ya);
dxa=0.02;
dya=0.02;
lengthX = xa(end);
lengthY = ya(end);
avg_single_rough = 0;
[X,Y] = size(g_initial);
for k = 1:Y
for l = 1:X
 avg_rough(l,k) = abs(g_initial(l,k));
 avg_single_rough = abs(g_initial(l,k))* dxa * dya + avg_single_rough;
end
```

```
end
avg_single_rough = avg_single_rough/(lengthY*lengthX)*r_scale
rough_ratio = avg_single_rough*100/d
rough_scale_factor = r / rough_ratio;
g_initial = g_initial * rough_scale_factor;
avg_single_rough = 0;
for k = 1:Y
for l = 1:X
 avg_rough(l,k) = abs(g_initial(l,k));
 avg_single_rough = abs(g_initial(l,k))* dxa * dya + avg_single_rough;
end
end
avg_single_rough = avg_single_rough/(lengthY*lengthX)*r_scale
agg_rough_sin_ratio = avg_single_rough*100/d
rms_rough = 0;
for k = 1:Y
for l = 1:X
 RoughRMS(l,k) = g_initial(l,k)^2;
 rms_rough = g_initial(l,k)^2 * dxa * dya + rms_rough;
end
end
rms_rough = sqrt(rms_rough/(lengthX*lengthY))*r_scale
rough_rms_m = mean(rms(g_initial))*r_scale
rms_rough = rms_rough/r_scale;
sk = 0;
su = 0;
for k = 1:Y
for l = 1:X
 sk = g_initial(l,k)^3 * dx * dy + sk;
 su = g_initial(l,k)^4 * dx * dy + su;
end
end
sk = sk/(rms_rough^3 * lengthX*lengthY)
su = su/(rms_rough^4 * lengthX*lengthY)
p = zeros(3,length(x),length(y)); %points required for nrbmak
for l=1:length(y)
 p(1,:,l) = x;
for k=1:length(x)
 p(2,k,l) = y(l);
 p(3,k,l) = g_initial(k,l);
end
end
```

ii) MATLAB code to obtain 3D irregular cylindrical surface

```
clear all
clc
format bank
% z=0:1:12;
 a=0.00123; b=0.00129;
% %c=rand(length(d),length(theta));
% % for i=1:length(d)
%    for j=1:length(theta)
%    r(i,j)=c(i);
%       %r(i,j)= theta(i)*.2;
%    z(i,j)=theta(i)*1;
%    end
% end
% r
% z
theta = (0:10:360)'; %angle variation from 0 to 2*pi
%d = 0:0.5:50'; %space of 0.5 cm to vary the radius
%d=2+3*randn(101,1)';
d=linspace(0,50,60);
variation_per=[0.01 0.02 0.03 0.04 0.05];
%r_var = a+(b-a)*(rand(length(theta)-1,length(d))); %random radius between 121 and
123
for i=1:length(variation_per)
r_var=a+variation_per(i)*a*(rand(length(theta)-1,length(d)));
r_var(end+1,:) = r_var(1,:);
x=r_var.*cosd(theta);
y=r_var.*sind(theta);
%z=cos(50*atan2(y,x)).* sin(100*atan2(y,x)).*exp(atan2(y,x).^2);
z=repmat(ones(size(theta)).*d,1);
%subplot(3,2,i)
figure(i)
surf(x,y,z);grid on;
% title('Cylindrical surface')
%plot(x,y);grid on; title('Cross Sectional Surface')
%figure(1);plot(x,y);grid on; title('Cross Sectional Surface')
%figure(2);surf(x,y,z);grid on; title('Cylindrical surface')
%pause
title(sprintf('cylindrical surfce with radius variation(in percentage)= %d', i));
figure(i+length(variation_per))
plot(x,y);grid on;
%title('Cross Sectional Surface')
title(sprintf('Cross sectional Surface of cylinder with variation in radius(in
percentage)= %d', i));
end
% header={'x','y','z'};
% xlswrite('E:\subu code\cylindricaldata.xlsx',[x(:),y(:),z(:)],'sheet1','A2');
% xlswrite('E:\subu code\cylindricaldata.xlsx',header,'Sheet1','A1');
```

(iii) Matlab Code for polynomial curve fitting

```
clc
%format compact
%format bank
format longe
%format bank
%format compact
[data_sim,txt]=xlsread('data_sim.xlsx');
x=data_sim(:,1); % data for the Reynold Number
y=data_sim(:,2); % Simulated value of the Nusselt Numbet
c=data_sim(:,6); % Analytical Calculation of the Nusselt Number
n=2; %order of the polynomial
z=polyfit(x,y,n); %Polynomial for the curve fitting
p=polyval(z,x); % value of the polynomial for different Reynold Number
fitt_err=y-p; % error for the polynomial curve fitting
calc_simul=c-y; % error between the calculated and simulated value
clc
figure (1);plot(x,y,'b',x,p,'ko'); grid on; xlabel('Reynolds Number[Re]');
ylabel('Nusselt Number[Nu]');
legend('Simulation Data','Fitted Polynomial Model')
figure (2);plot(x,y,'b',x,c,'ko'); grid on;
legend('Simulated Data','Calculated Data'); xlabel('Reynolds Number[Re]');
ylabel('Nusselt Number[Nu]');
figure(3); axis('equal')
plot(x,fitt_err,'k'); grid on; title('error between simulated and Fitted Value');
legend('error'); xlabel('Reynolds Number[Re]');ylabel('error');
figure (4)
plot(x,calc_simul,'k'); grid on; title('error between Calculated and simulated value');
legend('error'); xlabel('Reynolds Number[Re]');ylabel('error');
rms_fitted=sqrt(mean((y-p).^2));
rms_per_fit=rms_fitted*100
rms_calc_sim=sqrt(mean(c-y).^2);
rms_per_calc_sim=rms_calc_sim*100
fprintf('Root Mean Square for the fitted data and the simulated value (in percent) is :
%g\n',rms_per_fit)
fprintf('Root Mean Square for the Calculated and the simulated value (in percent) is :
%g\n',rms_per_calc_sim)
```